UTSUNOMIYA UNIVERSITY

# Enhancement approach of Mueller matrix Polarimeter

By
Kaustav Bhattacharyya

A thesis for the
Degree of Doctor of Philosophy

in the
Faculty of innovation system Engineering

March 2020

# Enhancement approach of Mueller matrix Polarimeter

**KAUSTAV BHATTACHARYYA**

**Advisor:**

Prof. Yukitoshi Otani

**Co-Advisors:**

Prof. Yoshiyo Hayasaki

Prof. Noboru Yugami

**Project advisors:**

Prof. Miyoshi Ayama

Prof. Hirotsugu Yamamoto

**Defense Committee Members:**

Prof. Yoshiyo Hayasaki

Prof. Noboru Yugami

Prof. Okihiro Sugihara

Prof. Ryushi Fujimura

# Declaration of Authorship

I, Kaustav Bhattacharyya, declare that I have authored this thesis titled**.** 'Enhancement approach of Mueller matrix Polarimeter' independently and the work presented in it is my original work.

I confirm that this work was done wholly or mainly while in candidature for a research degree at Utsunomiya University. It contains no materials previously published or written by another person**,** nor material which to a substantial extent has been accepted for the award of any other degree or diploma of the university or other institutes of higher learning, except where due acknowledgment has been made in the text.

Signed:

Date:

“It is the study of optics, which has enlightened my life…..”

# Abstract

This research work is on the enhancement of Mueller matrix polarimeter. The enhancement is achieved in two aspects- i) enhancement of accuracy and ii) enhancement of time. In the first method**,** enhancement of accuracy is obtained by calibration of the errors due to non-ideal retarders of a dual rotating retarder Mueller matrix polarimeter. The dual rotating retarder polarimeter was proposed initially by Azzam. It is composed of two rotating retarders and two fixed polarizers with the final purpose of retrieving the Mueller matrix of a sample. As the Algorithm used for calibration of the retardation and the azimuthal errors already exist, we propose to take into account the diattenuation errors of the two retarders along with the retardance errors. When the retarders of a dual rotating retarder polarimeter rotate at a rate of 5:1, we can obtain the 25 coefficients by Fourier transform of the output signal. From this Fourier coefficient, the Mueller matrix of the sample can be obtained. The calibration for the retardance and diattenuation errors has been done by no sample experiment method. As the Mueller matrix of air is known, the value of the retardance and diattenuation can be retrieved from the Fourier coefficients of the output signal. The algorithm has been described and the accuracy of the method has been tested with supporting experimental results and then compared with other existing method also. In the second method**,** enhancement of time is obtained by construct single shot Mueller matrix polarimeter using the property of channelled spectrum and axially symmetric quarter waveplate. A circular grating has been used here instead of conventional grating. Mueller matrix polarimeter is constructed by modulating the polarizing state of the input beam into polarizing state generator and also analysing the polarizing state of the output beam by polarizing state analyser. This modulation is generally done by modulation in the time domain, modulation in the spatial domain, modulation in the spectral domain. But to construct a single shot Mueller matrix polarimeter using this kind of modulation is a little difficult. Here we have proposed to construct a single shot Mueller matrix polarimeter using the combination of spatial domain modulation and spectral domain modulation of polarization. For spatial domain modulation of polarization, an achromatic axially symmetric wave plate (AASWP) has been used. Achromatic axially symmetric wave plate (AASWP) acts like a Fresnel rhomb and introduces the phase differences between the two axes of the beam. Thus it behaves like a retarder where retardance remains constant but the fast axis orientation varies over the

space. For spectral domain modulation, the theory of channelled spectrum has been adopted and, therefore, two high order retarders and a polarizer have been used. When broadband wavelength light passes through high order retarder, the retarder introduces different phase for each wavelength. By using a grating, these wavelengths can be separated, and modulation over the space can be measured. For the grating, a circular or radial grating has been used. This is a tricky thing for this proposal. Generally, gratings are linear or crossed, but here circular grating is used to separate the wavelengths radially.

# Acknowledgments

I am immensely grateful to my Research Advisor, Prof. Yukitoshi Otani, Centre of Optical Research and Education (CORE), Utsunomiya University for allowing me the opportunity to do the Ph.D. research work under his esteemed guidance. I owe my profound gratitude to Prof. Otani for his magnanimous support, patronage, tutelage, innovative discussions, scholarly advice and valuable suggestions given throughout my career of research, which incented me to widen my knowledge in polarization field and stimulated me in my Ph.D. research work. Sir supported me continuously in my research work, writing scientific papers and made sure the work progressing well. I could not have imagined having a better Research Advisor and mentor for my research work and I deem it my privilege to work under his able guidance.

Besides my Research Advisor, I would like to thank my Ph.D. Dissertation Committee Members, for their valuable suggestions, insightful comments, and encouragement that helped me conduct the research.

I am very thankful to Prof. Nathan Hagen, Centre of Optical Research and Education (CORE), Utsunomiya University, and Prof. Toshitaka Wakayama, School of Biomedical Engineering Saitama Medical University for their support in my research work.

I am also indebted to the Ministry of Education Culture, Sports, Science, and Technology, Govt. of Japan (MEXT) for providing me the 'Monbukagakusho' Fellowship to undertake this research in Japan. Without their precious support, it would not be possible to conduct this research.

Finally, I place on record my sincere thanks to all faculty members of CORE for supporting me during my entire research period. Special thanks to all of my colleagues of CORE for their cooperation and aid. I count myself lucky to work with them. Their incredible love, support, and wonderful companionship will forever be treasured in my life.

## Funding

This research was supported by the Ministry of Education Culture, Sports, Science and Technology, Government of Japan (MEXT) for the scholarship support.

Thanks to the Center for Optical Research and Education, CORE and the Innovation System Department of Utsunomiya University for supporting me with a Research Assistance scholarship.

# Contents

# List of Figures

# List of Tables

# Abbreviations

FFT - Fast Fourier Transform

DOP - Depth of Polarization

M - Mueller matrix

S- Stokes vectors

PSG - Polarization state generator

PSA - Polarizing state analyzer

T - Intensity transmittance

# Symbols

◦ - Degree
cm - Centimeter
λ - Lamda
θ- Theta
Φ- Phi
π- Pi
μm - Micrometer
i - Imaginary coefficient in complex number
E - Electric field vector
H - Magnetic field vector

*Dedicated to my loving mother & sister, and my teachers*

## Purpose

Mueller matrix is widely used not only in optical research, but also has an implementation in biomedical and bio-optics research to analyze several physical parameters such as the chiral nature of bio-molecules, sugar concentration of a solution, three-dimensional characteristics of the chemical bond, cancer diagnosis**,** and many others [1-15].

The research work is on the enhancement of Mueller matrix polarimeter; enhancement of accuracy**,** and enhancement of time. For enhancement of accuracy, we propose to calibrate the errors due to non-ideal retarders of a dual rotating retarder Mueller matrix polarimeter. The algorithm has been described and the accuracy of the method has been shown with supporting experimental results. For enhancement of time**,** we propose to construct a single shot Mueller matrix polarimeter using the property of channelled spectrum and axially symmetric quarter waveplate. A circular grating has been used here instead of conventional grating. The proposed theoretical approach is described with a supporting algorithm.

The research work is on the enhancement of Mueller matrix polarimeter. The enhancement is achieved by two methods - enhancement of accuracy and enhancement of time.

In the first method, enhancement of accuracy is obtained by calibrating the errors due to non-ideal retarders of a dual rotating retarder Mueller matrix polarimeter. The dual rotating retarder polarimeter was proposed initially by Azzam [1]. It is composed of two rotating retarders and two fixed polarizers with the final purpose of retrieving the Mueller matrix of a sample. *As the Algorithm used for calibration of the retardation and the azimuthal errors already exist, we propose to take into account the diattenuation errors of the two retarders along with the retardance errors. When the retarders of a dual rotating retarder polarimeter rotate at a rate of 5:1, we can obtain 25 coefficients by Fourier transform of output signal. From this coefficient the Mueller matrix of the sample can be obtained.

The calibration for the retardance and diattenuation errors has been done by no sample experiment method. As the Mueller matrix of air is known, the value of the retardance and diattenuation can be retrieved from the Fourier coefficients of the output signal.

The algorithm has been described and the accuracy of the method has been shown with supporting experimental results with other comparative methods also.

In the second method enhancement of time is obtained by construct a single shot Mueller matrix polarimeter using the property of channelled spectrum and axially symmetric quarter waveplate. A circular grating has used here instead of conventional grating.

Mueller matrix polarimeter is constructed by modulating the polarizing state of the input beam in polarizing state generator and also analysing the polarizing state of the output beam in polarizing state analyser. This modulation is generally done by modulation in the time domain, modulation in the spatial domain, modulation in the spectral domain. But to construct a single shot Mueller matrix polarimeter using this kind of modulation is a little difficult.

Here we have proposed to construct a single shot Mueller matrix polarimeter using the combination of spatial domain modulation and spectral domain modulation of polarization.

For spatial domain modulation of polarization, an achromatic axially symmetric wave plate (AASWP) has been used. Achromatic axially symmetric wave plate (AASWP) act like a Fresnel rhomb and introduce phase difference between the two axes of the beam. So that it behaves like a retarder where retardance remains constant but the fast axis orientation varies over the space.

For spectral domain modulation, the theory of channelled spectrum has been adopted and, therefore, two high order retarders and a polarizer have been utilised. When broadband wavelength light passes through high order retarders, the retarders introduce different phase for each wavelength. By using a grating, these wavelengths can be separated and modulation over the space can be measured.

For the grating, a circular or radial grating has been used. This is a tricky thing for this proposal. Generally, gratings are linear or crossed, but here circular grating is used to separate the wavelengths radially.

# 1. Introduction

Light is an electromagnetic wave. The electric and magnetic fields remain perpendicular to the propagation of light. In practical cases, the magnetic field is ignored as it does not hold any significant meanings. When the electric field remains in a particular manner, the light is treated as polarized light.

## 1.1 Polarization of light

Under normal atmospheric conditions, it has been well established that light can be treated as an electromagnetic wave. Light consists of both electric and magnetic waves and therefore has inherent magnitude and phase for each. In terms of the science of polarization and the property of light to be polarized, the magnetic vector is ignored, as it holds no bearing on the polarization phenomenon. Therefore, in discussing the principle of polarization only the electric field of light will be of value. Light is also considered a transverse electromagnetic wave meaning that the medium is displaced in a direction perpendicular to the motion of the wave.

When light is polarized only in the horizontal direction it is called horizontally polarized (H), when in the vertical direction it is called vertically polarized (V). There are many other kinds of polarizations viz. circular polarization (both left & right), elliptical polarization, etc. And when the polarization state changes randomly, it is termed as unpolarized light.

Natural light is termed unpolarized, which has been thought of as a misnomer. Light always has a polarization state; however, natural light has a very fast oscillating polarization state, and, therefore, it appears not to prefer any distinct polarization state. It can be thought of as containing all polarization states over a very short period of time, therefore, undetectable by modern detection systems.

## 1.2 The Stokes parameter

The modern representation of polarized light actually had its origin in 1852 by G. G. Stokes, who introduced 4 quantities that are functions only of observables of the electromagnetic waves and known as Stokes parameters; they are $S_0$, $S_1$, $S_2$, &$S_3$.

Mathematically, light can be thought of as two orthogonal electric waves oscillating at the same frequency. The set of equations (1) below describes the electric field of monochromatic light propagating in free space (which is by definition polarized). The relation between Stokes vectors and Mueller matrix is shown in Fig. 2.1.

$$E_x = E_{0x} \exp(i\delta)$$
$$E_y = E_{0y} \exp(i\delta) \qquad 1.1$$

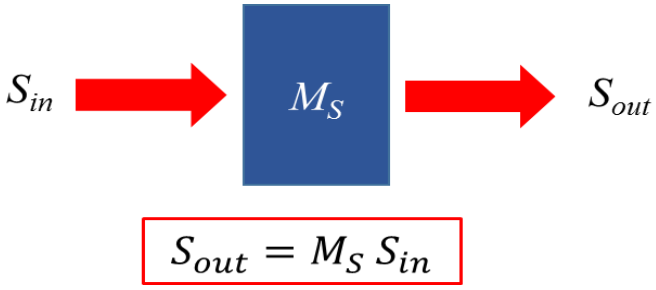


Fig. 2.1 Relation between output and input stokes vector

The Stokes parameters are defined by the following equations,

$$S = \begin{pmatrix} S_0 \\ S_1 \\ S_2 \\ S_3 \end{pmatrix} = \begin{pmatrix} E_{0x}^2 + E_{0y}^2 \\ E_{0x}^2 - E_{0y}^2 \\ 2\,E_{0x}E_{0y}\cos\delta \\ 2\,E_{0x}E_{0y}\sin\delta \end{pmatrix} = \begin{pmatrix} I \\ I_H - I_V \\ I_P - I_M \\ I_R - I_L \end{pmatrix} \qquad 1.2$$

Where I is the measured intensity value, $S_0$ is the total detected light intensity, of which $S_1$ is the portion that corresponds to the difference between linear horizontal and vertical polarization states, $S_2$ is the portion that corresponds to the difference between the linear +45° and –45° polarization states, and $S_3$ is the portion that

corresponds to the difference between the right circular and left circular polarization states. In this equation, I is the detected intensity represented with a subscript for the polarization type it represents (H=horizontal, V=vertical, P= +45º, M=45º, R= right circular, and L= left circular). These measured intensities translate into the Stokes values. All of the values lie between -1 and 1.

The relation between stokes parameters is,

$$S_0^2 \geq S_1^2 + S_2^2 + S_3^2 \qquad 1.3$$

Where the = and > indicate completely and partially/depolarized light.
The Depth of Polarization (DOP) is defined as,

$$DOP = \frac{\sqrt{S_1^2 + S_2^2 + S_3^2}}{S_0} \qquad 1.4$$

The DOP is 1 for completely polarized light, zero for totally depolarized light, and assumes a fractional value for any case in between.

The optical states of Stokes vectors are shown in Fig. 2.2.

$$S = \begin{bmatrix} S_0 \\ S_1 \\ S_2 \\ S_3 \end{bmatrix}$$

$$S_H = \begin{bmatrix} 1 \\ 1 \\ 0 \\ 0 \end{bmatrix}$$

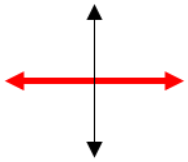

$$S_V = \begin{bmatrix} 1 \\ -1 \\ 0 \\ 0 \end{bmatrix}$$

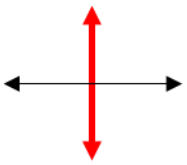

$$S_{45} = \begin{bmatrix} 1 \\ 0 \\ 1 \\ 0 \end{bmatrix}$$

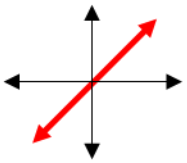

$$S_R = \begin{bmatrix} 1 \\ 0 \\ 0 \\ 1 \end{bmatrix}$$

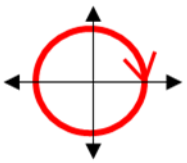

2.2 Stokes vector parameters

## 1.3 MUELLER MATRIX

In 1943, Hans Mueller developed a matrix that relates the Stokes vector of the light impinging on a sample to the Stokes vector leaving the sample. Using the method with the input and output polarization states (Stokes vectors) known, the 4x4 Mueller matrix can be used to describe the polarization properties of a sample. This relationship is shown below in where M is the Mueller matrix and $S_{out}$ and $S_{in}$ are the output and input Stokes vectors respectively.

$$S_{out} = M_s . S_{in} \tag{1.5}$$

$$\begin{bmatrix} S_0 \\ S_1 \\ S_2 \\ S_3 \end{bmatrix}_{out} = \begin{bmatrix} m_{11} & m_{12} & m_{13} & m_{14} \\ m_{21} & m_{22} & m_{23} & m_{24} \\ m_{31} & m_{32} & m_{33} & m_{34} \\ m_{41} & m_{42} & m_{43} & m_{44} \end{bmatrix} . \begin{bmatrix} S_0 \\ S_1 \\ S_2 \\ S_3 \end{bmatrix}_{in} \tag{1.6}$$

Mueller matrix information is arranged in a 4x4 matrix which describes the optical properties of an element. The Mueller matrix can be decomposed in three polarization properties known as diattenuation, retardance and depolarization and each of these with its own more specific properties [6,7].

The Mueller matrix parameters are shown in Fig. 2.3.

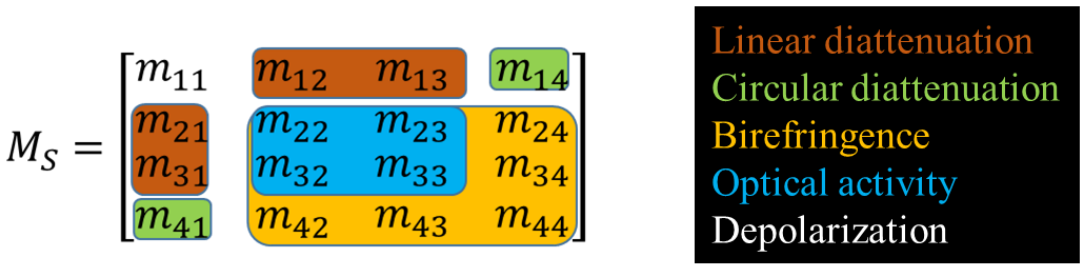


Fig. 2.3 Muller matrix parameters

Each of these properties can be associated on physical properties of the sample, only to mention some: The linear and circular diattenuation can be associated with the scattering and chirality measurement; the circular retardance is helpful for glucose measurement; birefringence can be associated with stress analysis and from depolarization properties some cancer diagnosis can be done [7,8].

Mueller matrix is widely used not only in optical research**,** but also has an implementation in biomedical and bio-optics research to analyze several physical parameters such as chiral nature of bio-molecules, sugar concentration of a solution, three dimensional characteristics of the chemical bond, cancer diagnosis**,** and many others [9-15].

The parameters that we can measure by Mueller matrix are:

- Depolarization, from which cancer can be detected.
- Linear diattenuation, used for scattering measurement.
- Birefringence, commercially used for stress analysis.
- Circular retardance, used for glucose measurement.
- Circular diattenuation, used for chirality analysis.

The optical parameters and the physical parameters obtained from these are shown in Fig. 2.4.

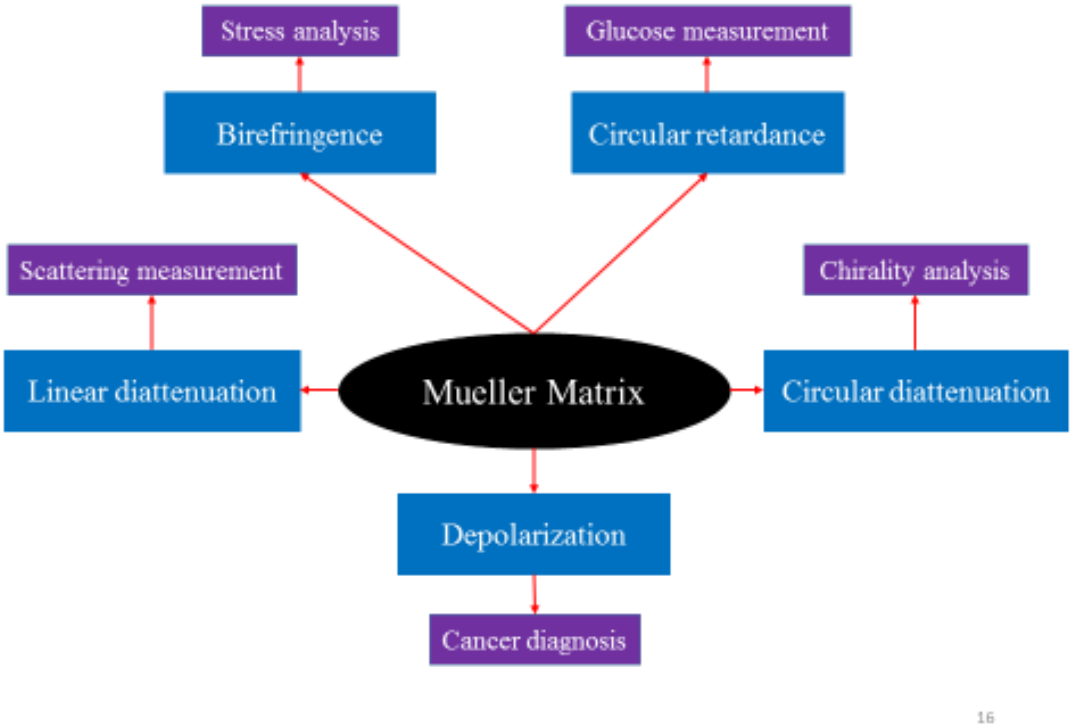


Fig. 2.4 Physical properties of Muller matrix parameter

# 2 Mueller matrix Polarimeter

Mueller matrix polarimeter is a device that measures the Mueller matrix of a sample using polarizing state generator (PSG) and polarizing state analyzer (PSA). Polarizing state generator creates various states of polarization of the input beam, whereas polarizing state analyzer analyzes various states of polarization.

Mueller matrix polarimetry is an experimental technique to determine the optical properties of a sample by measuring its Mueller matrix. It measures the Mueller matrix of the sample by producing various polarization states in the input beam and analyzing various states of the output beam.

Several Mueller matrix polarimeter designs can be found in the literature, the main difference is in the polarization state generator/analyzer composition, i.e. dual rotating retarders [1,2], couple phase modulators [3] and liquid crystal devices [4,5]. More specifically, in the dual rotating retarder implementation**,** a fixed polarizer and a rotating retarder compose the polarization state generator (PSG) to produce various polarizing state in the input, and a rotating retarder and a fixed analyzer in the polarizing state analyzer (PSA) to detect various polarization state at the output beam[1,2].

A simple layout of Mueller matrix polarimeter has been shown below Fig.2.5:

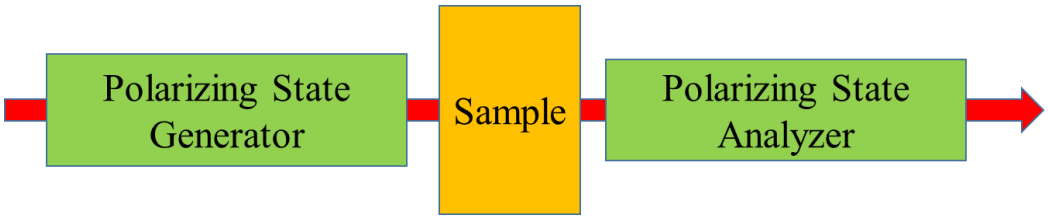


Fig. 2.5 Block diagram of Mueller matrix polarimeter.

## 2.1 Motivation and challenges

Mueller matrix is widely used not only in optical research, but also has an implementation in biomedical and bio-optics research to analyze several physical parameters such as chiral nature of bio-molecules, sugar concentration of a solution, three-dimensional characteristics of the chemical bond, cancer diagnosis, and many others [9-15].

The research work is on the enhancement of Mueller matrix polarimeter; enhancement of accuracy and enhancement in time. For enhancement of accuracy**,** our proposal is to calibrate the errors due to non-ideal retarders of a dual rotating retarder Mueller matrix polarimeter. The algorithm has been described and the accuracy of the method has been shown with supporting experimental results. For enhancement in time**,** our proposal is to construct a single shot Mueller matrix polarimeter using the property of channelled spectrum and axially symmetric quarter waveplate. A circular grating has been used here instead of conventional grating. The proposed theoretical approach is described with a supporting algorithm.

## 2.2 Relationship to existing approaches

Several Mueller matrix polarimeter can be found in the literature, the main difference is in the polarization state generator/analyzer composition, i.e. dual rotating retarders [1][2], couple phase modulators [3] and liquid crystal devices [4][5]. More specifically, in the dual rotating retarder implementation**,** a fixed polarized and a rotating retarder composes the polarization state generator (PSG) to produce various polarizing state in the input, and a rotating retarder and a fixed analyzer in the polarizing state analyzer (PSA) to detect various polarization state at the output beam[1][2].

Mueller matrix is widely used not only in optical research, but also has an implementation in biomedical and bio-optics research to analyze several physical parameters such as chiral nature of bio-molecules, sugar concentration of a solution, three dimensional characteristics of the chemical bond, cancer diagnosis**,** and many others [6-12].

Mueller matrix information is arranged in a 4x4 matrix which describes the optical properties of an element. The Mueller matrix can be decomposed in three polarization properties known as diattenuation, retardance and depolarization and each of these with its own more specific properties [13]. Each of these properties can be associated on physical parameters of the sample, only to mention some: The linear and circular diattenuation can be associated with the scattering and chirality measurement; the circular retardance is helpful for glucose measurement; birefringence can be associated with stress analysis and from depolarization properties some cancer diagnosis can be done [14][15].

To increase the accuracy of a polarimeter**,** it is necessary to compensate the errors caused by some of the components used. The systematic errors can be caused due to the retardance and diattenuation properties of the components, non-uniform rotation of retarders stage, intensity fluctuation of the light source, the broadband wavelength of the light, the wavelength dependency of the retarders, etc. Several researches have already been done to compensate most of these errors [16-21]. Generally, retarders' properties are the main source of errors that can be compensated by taking a non-ideal component.

# 3 Enhancement of accuracy of Mueller matrix polarimeter

To increase the accuracy of a polarimeter**,** it is necessary to compensate the errors caused by some of the components used. In the dual rotating retarder Mueller matrix measurement method, the systematic errors can be caused due to the retardance and diattenuation properties of the components, non-uniform rotation of retarders stage, intensity fluctuation of the light source, the broadband wavelength of the light, the wavelength dependency of the retarders, etc. Several researches have already been done to compensate most of these errors [16-21]. The dual rotating retarder polarimeter was initially proposed by Azzam in 1978 [1]. The calibration for retardance and azimuthal errors of this system was done by Goldstein and Chipman in 1990 [16]. After this**,** some more calibration has been done [18-20].

Generally, the main source of error occurs due to non-ideal retarder which needs to be compensated. Although retarder is considered as a wave plate, sometimes it has diattenuation value that can cause errors for precise and high accurate measurement to study the polarization properties of the sample. Our proposed method is to compensate the diattenuation and retardation errors of the retarders to enhance the accuracy of the system that has been presented with supporting experimental results.

In addition, to do enhancement in time of Mueller matrix polarimeter, our proposal is to construct a single shot Mueller matrix polarimeter using the property of channelled spectrum and axially symmetric quarter waveplate [23][24]. A circular grating has used here instead of conventional grating. The proposed set up has been described with a supporting algorithm.

Here we have proposed to construct a single shot Mueller matrix polarimeter using the combination of spatial domain modulation and spectral domain modulation of polarization.

For spatial domain modulation of polarization, an achromatic axially symmetric wave plate (AASWP) has been used [24]. Achromatic axially symmetric wave plate (AASWP) act like a Fresnel rhomb and introduce phase difference between

the two axes of the beam. So that it behaves like a retarder where retardance remains constant but the fast axis orientation varies over the space.

For spectral domain modulation, the theory of channelled spectrum has been adopted [23] and thus two high order retarders and a polarizer have been used. When broadband wavelength light passes through high order retarder, the retarder introduces different phase for each wavelength. By using a grating these wavelengths can be separated and modulation over the space can be measured.

For the grating, a circular or radial grating has been used. This is a tricky thing for this proposal. Generally, gratings are linear or crossed, but here circular grating is used to separate the wavelengths radially.

The two methods have been used for the enhancement of Mueller matrix polarimeter is shown in Fig. 2.6.

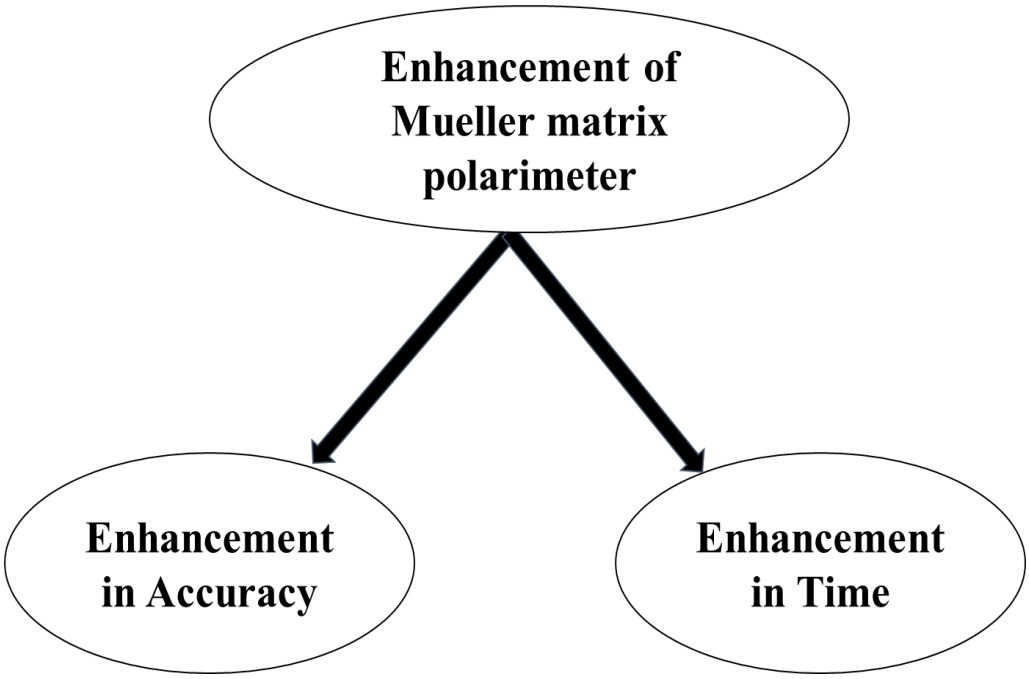


Fig. 2.6 Two ways have been used for enhancement of Mueller matrix polarimeter

## 3.1 Dual-Rotating Retarder Polarimeter

The dual rotating retarder polarimeter, Fig3.1, consists of a polarization state generator (PSG) and a polarization state analyzer (PSA), each composed by a fixed polarizer ($M_P$,$M_A$) and a rotating retarder ($M_R(\theta)$, $M_R(5\theta)$ respectively). When the retarder of the PSA and the PSG rotates with an angular velocity 5:1, its output signal generates 12 harmonic frequencies in the Fourier spectrum. The Mueller matrix elements of the sample are retrieved from its Fourier complex coefficients [1] [2].

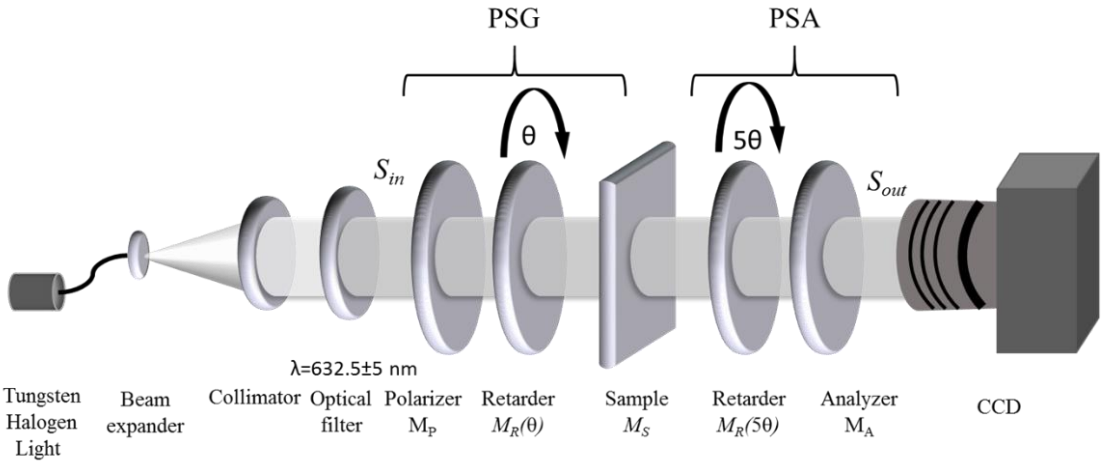


Fig 3.1 Dual rotating retarder polarimeter.

The output stokes vector will be:

$$S_{out} = \begin{bmatrix} S_0 \\ S_1 \\ S_2 \\ S_3 \end{bmatrix}_{out} = \left[M_A\, M_R\,(5\theta) M_S M_R(\theta) M_p\right] \cdot S_{in} \qquad 3.1$$

Where $M_S$ is the Mueller matrix of the components, $\theta$ and $5\theta$ is the rotation of the PSG and PSA retarder respectively. $M_R(\theta)$ is the Mueller matrix of a quarter-wave retarder oriented at an angle $\theta$, and $M_P$ and $M_A$ is the Mueller matrix of a horizontally linear polarizer, given by [22]:

$$M_R(\theta) = \begin{bmatrix} 1 & 0 & 0 & 0 \\ 0 & cos^2 2\theta & sin2\theta\, cos2\theta & -sin2\theta \\ 0 & sin2\theta\, cos2\theta & sin^2 2\theta & cos2\theta \\ 0 & sin2\theta & -cos2\theta & 0 \end{bmatrix} \quad 3.2$$

$$M_P = M_A = \begin{bmatrix} 1 & 1 & 0 & 0 \\ 1 & 1 & 0 & 0 \\ 0 & 0 & 0 & 0 \\ 0 & 0 & 0 & 0 \end{bmatrix} \quad 3.3$$

By making the matrix multiplication with the Mueller matrix of the sample, Eq. (3.1), the output intensity captured by the detector can be represented as:

$$S_{0\,out} = \mu_{11}m_{11} + \mu_{12}m_{12} + \mu_{13}m_{13} + \cdots\cdots\cdots + \mu_{44}m_{44} \quad 3.4$$

Where $m_{ij}$ are the elements of Mueller matrix of the sample, and $\mu_{ij}$ are the corresponding coefficients dependent on the angular position of the retarder $\theta$**,** the output intensity can be expressed in the form of a Fourier series as:

$$S_{0\,out} = a_0 + \sum_{n=1}^{12} \left(a_n\, cos2n\theta + \, b_n\, sin2n\theta\right) \quad 3.5$$

Where $a_n$ and $b_n$ are the real and imaginary Fourier coefficients.

From the inverse calculation, the elements of the Mueller matrix of the sample are successfully determined by [1][2]:

$$
\begin{aligned}
m_{11} &= \left( a_0 - a_2 + a_8 - a_{10} + a_{12} \right) \\
m_{12} &= 2\left( a_2 - a_8 - a_{12} \right) \\
m_{13} &= 2\left( b_2 + b_8 - b_{12} \right) \\
m_{14} &= \left( b_1 + b_9 - b_{11} \right) \\
m_{21} &= 2\left( a_{10} - a_8 - a_{12} \right) \\
m_{22} &= 4\left( a_8 + a_{12} \right) \\
m_{23} &= 4\left( b_{12} - b_8 \right) \\
m_{24} &= 4\left( b_{11} - b_9 \right) \\
m_{31} &= \left( b_{10} - b_8 - b_{12} \right) \\
m_{32} &= 4\left( b_8 + b_{12} \right) \\
m_{33} &= 4\left( a_8 - a_{12} \right) \\
m_{34} &= 2\left( a_9 - a_{11} \right) \\
m_{41} &= \left( b_3 + b_7 - b_5 \right) \\
m_{42} &= -2\left( b_3 + b_7 \right) \\
m_{43} &= 2\left( a_7 - a_3 \right) \\
m_{44} &= \left( a_6 - a_4 \right)
\end{aligned}
\qquad 3.6
$$

## 3.2 Implementation of diattenuation error

The dual rotating retarder polarimeter, Figure 3.2, consists of a polarization state generator (PSG) and a polarization state analyzer (PSA), each composed by a fixed polarizer ($M_P$,$M_A$) and a rotating retarder ($M_R(\theta)$, $M_R(5\theta)$ respectively). When the retarder of the PSA and the PSG rotates with an angular velocity 5:1, its output signal generates 12 harmonic frequencies in the Fourier spectrum. The Mueller matrix elements of the sample are retrieved from its Fourier complex coefficients [4] [5].

The errors due to non-ideal quarter-wave retarders and the azimuthal angles of the retarders and analyzer have been addressed before [5][7]. Our approach is to take into account the errors due to the diattenuation of the retarders only, retardance values are obtained using Goldstein-Chipman-algorithm for complementation of the model.

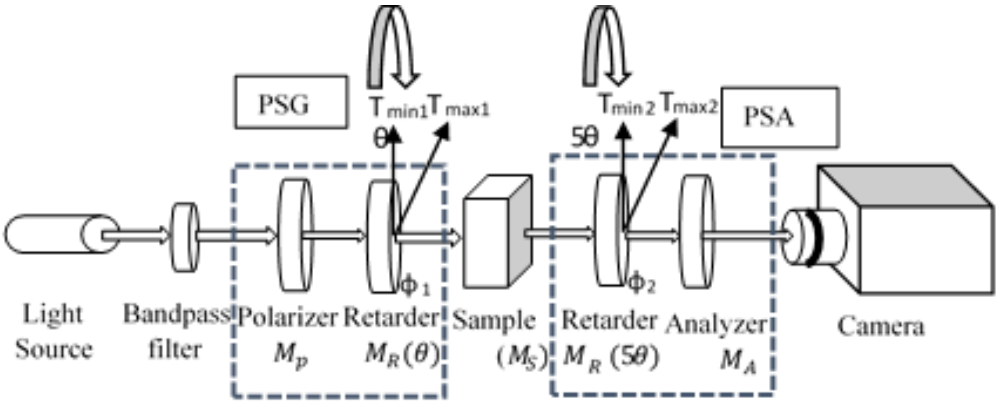


Figure 3.2. Dual rotating retarder polarimeter with diattenuation and retardation error of the retarder.

To get the Mueller matrix of the retarder with non-zero diattenuation characteristics, ($T_{max}$, $T_{min}$), and linear retardance $\phi$, its Mueller matrix is constructed by the matrix multiplication of a linear diattenuator, $M'_D$ ($\theta$, $T_{max}$, $T_{min}$) with a linear retarder $M'_R(\theta, \phi)$ given by [6][8]:

$$M'_{RD}(\theta,\phi,T_{max},T_{min}) = M'_R M'_D = M'_D M'_R =$$

$$\begin{bmatrix} (T_{max}+T_{min}) & (T_{max}-T_{min})cos2\theta & (T_{max}-T_{min})sin2\theta & 0 \\ (T_{max}-T_{min})cos2\theta & (T_{max}+T_{min})cos^2 2\theta + sin^2 2\theta cos\phi\, 2\sqrt{I_x I_y} & (T_{max}+T_{min}-cos\phi\, 2\sqrt{T_{max}T_{min}})sin2\theta\, cos2\theta & -sin2\theta sin\phi\, 2\sqrt{T_{max}T_{min}} \\ (T_{max}-T_{min})sin2\theta & (T_{max}+T_{min}-cos\phi\, 2\sqrt{I_x I_y})sin2\theta\, cos2\theta & (T_{max}+T_{min})sin^2 2\theta + cos^2 2\theta cos\phi\, 2\sqrt{T_{max}T_{min}} & cos2\theta sin\phi\, 2\sqrt{T_{max}T_{min}} \\ 0 & sin2\theta sin\phi\, 2\sqrt{T_{max}T_{min}} & -cos2\theta sin\phi\, 2\sqrt{T_{max}T_{min}} & cos\phi\, 2\sqrt{T_{max}T_{min}} \end{bmatrix} \quad (3.7)$$

Where, $T_{max}$ and $T_{min}$ are the maximum and minimum intensity transmittance of diattenuation, $\phi$ is the retardance of the retarder and $\theta$ is the angular orientation of the fast axis. By using the same procedure in the first sections, Eq. (1) and (3), but with the non-ideal retarders, its corresponding output Stokes vector will be given by:

$$S'_{out} = \left[M_A\, M'_{RD}\,(5\theta, \phi_2, T_{max2}, T_{min2}) M_S M'_{RD}(\theta, \phi_1, T_{max1}, T_{min1}) M_p\right] \cdot S_{in} \tag{3.8}$$

And

$$S'_{0\,out} = \mu'_{11} m_{11} + \mu'_{12} m_{12} + \mu'_{13} m_{13} + \cdots\cdots\cdots + \mu'_{44} m_{44} \tag{3.9}$$

Just as previously explained, Eq. (3.9), $m_{ij}$ are the elements of the Mueller matrix of the sample and $\mu'_{ij}$ are the corresponding coefficients dependent on the angular position of the retarder $\theta$. The output intensity can be expressed in the form of a Fourier series as [4][5]:

$$S'_{0\,out} = a_0 + \sum_{n=1}^{12} \left(a_n\, cos2n\theta + \, b_n\, sin2n\theta\right) \tag{3.10}$$

Following the same procedure explained in the introduction, where the Mueller matrix multiplication is done using Eq. (3.7-3.10), the Mueller matrix elements of the sample can be retrieved by the inverse calculation of the Fourier complex coefficients. In this case**,** the Mueller matrix coefficients will be dependent on diattenuation and retardation parameters of the retarders.

$$\begin{aligned}
m_{11} &= \frac{1}{p_1\, p_2 \alpha_2 \beta_1}\left[\alpha_2\beta_1 a_0 - \alpha_4\beta_1 a_2 + (\alpha_4\beta_2 + \alpha_2\beta_3 - \alpha_2\beta_4)\, a_8 - \alpha_2\beta_1\, a_{10} + (\alpha_4\beta_2 + \alpha_2\beta_3 - \alpha_2\beta_4)\, a_{12}\right] \\
m_{12} &= \frac{2}{\alpha_2\beta_1}(\beta_1 a_2 - \beta_2 a_8 - \beta_2 a_{12}) \\
m_{13} &= \frac{2}{\alpha_1\alpha_2}(\alpha_1 b_2 + \alpha_3 b_8 - \alpha_3 b_{12}) \\
m_{14} &= \frac{1}{sin\phi_1 p_2 z_1}\left(b_1 + \frac{2\alpha_3}{\alpha_1} b_9\right) \\
&\quad - \frac{p_2 q_1}{sin\phi_1\, p_1\, p_2 \alpha_1 \alpha_2\, p_2 z_1}\left[2\, p_1\, p_2 \alpha_1 b_2 + (4\, p_1\, p_2 - \alpha_4)\alpha_3 b_8 + \alpha_2\alpha_3 b_{10} - \alpha_3\alpha_4 b_{12}\right] \\
m_{21} &= \frac{2}{\alpha_1\beta_1}(\beta_1 a_{10} - \beta_3 a_8 - \beta_3 a_{12}) \\
m_{22} &= \frac{4}{\beta_1}(a_8 + a_{12})
\end{aligned} \tag{3.11}$$

$$m_{23} = \frac{4\,p_1 p_2}{\alpha_1 \alpha_2}(b_{12} - b_8)$$

$$m_{24} = -\frac{4\,p_1\,p_2}{sin\phi_1 \alpha_1 p_2 z_1} b_9 + \frac{2\,p_2\,q_1}{sin\phi_1 \alpha_1 \alpha_2 p_2 z_1}[(4\,p_1\,p_2 - \alpha_4)b_8 + \alpha_2 b_{10} - \alpha_4 b_{12}]$$

$$m_{31} = \frac{2}{\alpha_1 \alpha_2}(\alpha_2 b_{10} - \alpha_4 b_8 - \alpha_4 b_{12})$$

$$m_{32} = \frac{4\,p_1 p_2}{\alpha_1 \alpha_2}(b_{12} + b_8)$$

$$m_{33} = \frac{4\,p_1 p_2}{\alpha_1 \alpha_2}(a_8 - a_{12})$$

$$m_{34} = \frac{4\,p_1\,p_2}{sin\phi_1 \alpha_1 p_2 z_1} a_9$$

$$- \frac{2\,p_2\,q_1}{sin\phi_1 \alpha_1 \alpha_2 p_2 z_1 \beta_1}[(2\alpha_1\alpha_2 + 2\,p_1\,p_2\beta_1 - \alpha_2\beta_3)a_8 + \alpha_2\beta_1\,a_{10} - (2\,p_1\,p_2\beta_1 + \alpha_2\beta_3 - 2\alpha_1\alpha_2)a_{12}]$$

$$m_{41} = \frac{1}{sin\phi_2 p_1 z_2}\left(\frac{2\alpha_4}{\alpha_2} b_7 - b_5\right)$$

$$- \frac{p_1\,q_2}{sin\phi_2\,p_1\,p_2 \alpha_1 \alpha_2\,p_1 z_2}[\alpha_1\alpha_4 b_2 + \alpha_3\alpha_4 b_8 - 2\,p_1 p_2 \alpha_2 b_{10} + (4\,p_1 p_2 - \alpha_3)\alpha_4 b_{12}]$$

$$m_{42} = -\frac{4p_1\,p_2}{sin\phi_2 \alpha_2\,p_1 z_2} b_7 + \frac{2\,p_1\,q_2}{sin\phi_2 \alpha_1 \alpha_2\,p_1 z_2}[\alpha_1 b_2 + \alpha_3 b_8 + (4\,p_1\,p_2 - \alpha_3)b_{12}]$$

$$m_{43} = \frac{4\,p_1 p_2}{sin\phi_2 \alpha_2\,p_1 z_2} a_7$$

$$- \frac{2\,p_1 q_2}{sin\phi_2 \alpha_1 \alpha_2\,p_1 z_2 \beta_1}[\alpha_1\beta_1\,a_2 - (\alpha_1\beta_2 + 2\alpha_1\alpha_2 - 2\,p_1\,p_2\beta_1)a_8 + (2\,p_1\,p_2\beta_1 + 2\alpha_1\alpha_2 - \alpha_1\beta_2)a_{12}]$$

$$m_{44} = \frac{1}{sin\phi_1 sin\phi_2 z_1 z_2}\left[(a_6 - a_4) + \frac{4\,p_1 q_2}{\alpha_1} a_9 - \frac{4\,q_1 p_2}{\alpha_2} a_7 + \frac{4\,p_1 p_2 q_1 q_2}{\alpha_1 \alpha_2}(a_8 - a_{12})\right.$$

$$\left. + \frac{2\,q_1 q_2}{\alpha_1 \alpha_2 \beta_1}[\alpha_1\beta_1\,a_2 - (\alpha_1\beta_2 + 4\alpha_1\alpha_2 - \alpha_2\beta_3)a_8 - \alpha_2\beta_1\,a_{10} + (4\,p_1\,p_2\beta_1 + \alpha_2\beta_3 - \alpha_1\beta_2)a_{12}]\right]$$

For conveniences the parameters obtained were reduced by these relations:

$$T_{max1} + T_{min1} = p_1 \qquad T_{max2} + T_{min2} = p_2$$
$$T_{max1} - T_{min1} = q_1 \qquad T_{max2} - T_{min2} = q_2$$
$$2\sqrt{T_{max1}T_{min1}} = z_1 \qquad 2\sqrt{T_{max2}T_{min2}} = z_2$$

$$\begin{aligned}
\alpha_1 &= p_1(p_2 - cos\phi_2 z_2) & \beta_1 &= p_1p_2 - p_2cos\phi_1 z_1 - p_1cos\phi_2 z_2 + cos\phi_1 cos\phi_2 z_1 z_2 \\
\alpha_2 &= p_2(p_1 - cos\phi_1 z_1) & \beta_2 &= p_1p_2 - p_2cos\phi_1 z_1 + p_1cos\phi_2 z_2 + cos\phi_1 cos\phi_2 z_1 z_2 \\
\alpha_3 &= p_1(p_2 + cos\phi_2 z_2) & \beta_3 &= p_1p_2 + p_2cos\phi_1 z_1 - p_1cos\phi_2 z_2 + cos\phi_1 cos\phi_2 z_1 z_2 \\
\alpha_1 &= p_2(p_1 + cos\phi_1 z_1) & \beta_4 &= p_1p_2 + p_2cos\phi_1 z_1 + p_1cos\phi_2 z_2 + cos\phi_1 cos\phi_2 z_1 z_2
\end{aligned} \tag{3.12}$$

Were $T_{max1}$ , $T_{min1}$ , $T_{max2}$ and $T_{min2}$ as the maximum and minimum intensity transmission, $\phi_1$ and $\phi_2$ as the retardance of polarizing state generator and polarizing state analyzer retarder respectively.

The diattenuation ($D = \frac{T_{max} - T_{min}}{T_{max} + T_{min}}$) of the PSG and PSA retarders can be represented as:

$$D_1 = \frac{q_1}{p_1} \qquad D_2 = \frac{q_2}{p_2} \tag{3.13}$$

To calibrate the Mueller matrix polarimeter, the error constants of the proposed model can be retrieved by taking into account a no-sample measurement. In this case, the Mueller matrix can be taken ideally as an identity matrix and its corresponding output Stokes vector is given by:

$$S'_{0\,out} = \mu'_{11} + \mu'_{22} + \mu'_{33} + \mu'_{44} \tag{3.14}$$

Where $\mu'_{11}, \mu'_{22}, \mu'_{33}$ and $\mu'_{44}$ are the same equation parameters obtained in Eq. (3.9). The error constants can be retrieved from the Fourier coefficients:

$$p_1p_2 = a_0 - a_2 + a_8 - a_{10} \qquad p_1z_2 = \frac{2}{cos\phi_2}(a_2 - a_8)$$

$$q_1q_2 = 0.5\ (a_4 + a_6) \qquad p_2z_1 = \frac{2}{cos\phi_1}(a_{10} - a_8)$$

$$q_1p_2 = 0.5\ (a_1 + a_9) \qquad z_1z_2 = \frac{1}{2sin\phi_1 sin\phi_2}(3a_6 - a_4) \tag{3.15}$$

$$p_1q_2 = 0.5\ (a_3 + a_5)$$

$$\alpha_1 = a_0 - 3\ a_2 + 3\ a_8 - a_{10} \qquad \beta_1 = 4\ a_8$$

$$\alpha_2 = a_0 - a_2 + 3\ a_8 - 3\ a_{10} \qquad \beta_2 = 4\ a_2$$

$$\alpha_3 = a_0 + a_2 - a_8 - a_{10} \qquad \beta_3 = 4\ a_{10}$$

$$\alpha_4 = a_0 - a_2 - a_8 + a_{10} \qquad \beta_4 = 4\ (a_2 - a_8 + a_{10})$$

$$D_1 = \frac{0.5\ (a_1 + a_9)}{a_0 - a_2 + a_8 - a_{10}} \qquad D_2 = \frac{0.5\ (a_3 + a_5)}{a_0 - a_2 + a_8 - a_{10}}$$

$D_1$ and $D_2$ are the diattenuation of the PSG and PSA retarders respectively. The retardance of the retarder cannot be detected by this algorithm. To detect the retardance of the retarders we have used the Goldstein-Chipman-algorithm [5][7].

### 3.2.1 EXPERIMENTAL RESULTS

Experiments were done by using a tungsten halogen light source and a narrow band-pass filter of wavelength *632.5±5* nm. By using a *14* bit CCD camera (Thorlab-8050M-GE-TE), 36 images were taken covering a rotation of 180 degree, where each image was averaged by 20 frames for reducing noise. The obtained Mueller matrix by experiment is given below for various samples.

The average Mueller matrix value of *10×10* pixel at the center for various samples were measured and presented in Table 3.1. The results are compared with both the Goldstein-Chipman-algorithm [5][7] and our proposed algorithm.

Table 3.1. Experimental result of the Mueller matrix for various objects. Result obtained by two algorithms has shown with the theoretical values and without calibration result.

| Sample | Theoretical values | Without calibration | Goldstein-Chipman algorithm | Proposed algorithm |
|---|---|---|---|---|
| No Sample | $\begin{bmatrix}1&0&0&0\\0&1&0&0\\0&0&1&0\\0&0&0&1\end{bmatrix}$ | $\begin{bmatrix}1.000&0.000&-0.003&0.000\\0.049&0.947&0.001&0.008\\-0.009&-0.006&0.963&0.002\\-0.001&0.007&0.005&0.987\end{bmatrix}$ | $\begin{bmatrix}1.000&0.004&-0.008&0.000\\0.004&0.988&-0.015&0.008\\0.001&0.010&1.005&0.002\\-0.001&0.007&0.005&0.988\end{bmatrix}$ | $\begin{bmatrix}1.000&0.004&-0.003&-0.003\\0.004&0.994&0.001&0.014\\-0.009&-0.006&1.005&0.000\\0.003&0.000&0.003&1.002\end{bmatrix}$ |
| Quarter Wave Plate | $\begin{bmatrix}1&0&0&0\\0&1&0&0\\0&0&0&-1\\0&0&1&0\end{bmatrix}$ | $\begin{bmatrix}1.000&-0.043&0.011&0.006\\-0.031&0.997&0.014&-0.012\\0.005&-0.008&0.007&-0.982\\0.003&-0.010&0.930&0.008\end{bmatrix}$ | $\begin{bmatrix}1.000&-0.052&0.012&0.002\\-0.098&1.067&0.018&-0.006\\0.006&-0.003&0.008&-0.986\\0.006&-0.014&0.989&0.008\end{bmatrix}$ | $\begin{bmatrix}1.000&-0.052&0.011&0.002\\-0.094&1.063&0.015&-0.004\\0.006&-0.008&0.008&-0.996\\0.000&-0.004&0.983&0.015\end{bmatrix}$ |
| Linear Polarizer (Horizontal) | $\begin{bmatrix}1&1&0&0\\1&1&0&0\\0&0&0&0\\0&0&0&0\end{bmatrix}$ | $\begin{bmatrix}1.000&0.943&0.036&0.004\\1.032&0.922&-0.004&0.013\\-0.017&0.092&-0.091&-0.068\\-0.005&-0.026&0.025&-0.006\end{bmatrix}$ | $\begin{bmatrix}1.000&1.064&0.045&0.004\\1.048&1.062&-0.001&0.014\\-0.018&0.112&-0.104&-0.074\\-0.008&-0.032&0.029&-0.007\end{bmatrix}$ | $\begin{bmatrix}1.000&1.056&0.040&-0.019\\1.040&1.055&-0.005&0.061\\-0.024&0.105&-0.103&-0.063\\-0.028&0.037&0.032&-0.007\end{bmatrix}$ |
| Linear Polarizer (Vertical) | $\begin{bmatrix}1&-1&0&0\\-1&1&0&0\\0&0&0&0\\0&0&0&0\end{bmatrix}$ | $\begin{bmatrix}1.000&-0.969&-0.042&0.004\\-0.980&0.966&0.043&-0.004\\0.012&-0.017&0.010&0.047\\-0.006&0.007&0.015&0.009\end{bmatrix}$ | $\begin{bmatrix}1.000&-0.971&-0.044&0.004\\-0.981&0.968&0.044&-0.005\\0.006&-0.016&0.013&0.045\\-0.007&0.008&0.014&0.008\end{bmatrix}$ | $\begin{bmatrix}1.000&-0.977&-0.040&0.004\\-0.986&0.973&0.041&-0.005\\0.012&-0.016&0.012&0.038\\-0.004&0.002&0.000&0.008\end{bmatrix}$ |

To show the imaging capability and accuracy of the implemented system, the spatial distribution of Mueller matrix Fig 3.3(a) and its line profile along Y-axis Fig 3.3(b) for no sample measurement has been shown.

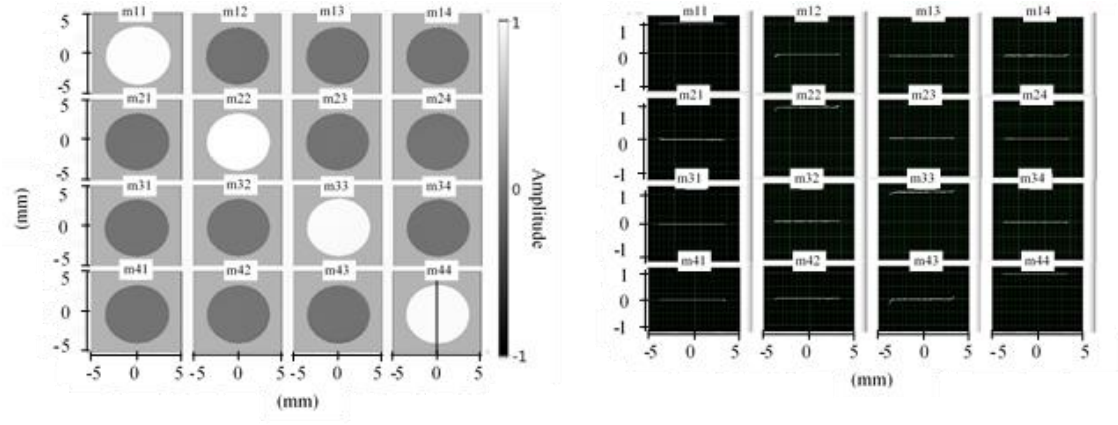


(a) The Mueller matrix image for no sample.

(b) Line profile of Mueller matrix along the central Y-axis (Marked in image m44).

Figure 3.3. Experimental images obtained for no sample. The Mueller matrix images and its one dimensional line profile along central Y axis has shown for the variation obtained.

Taking a quarter waveplate as a sample, its corresponding Mueller matrix images are presented in Fig 3.4(a) and its line profile along Y axis in Fig 3.4(b). All the line profiles are taken in the same position, which shows noise in the same position. This noise is due to the dust particles on the surface, improper polarizing property of the sample and defocus obtained by the imaging system. In these parts, the authors are urrently working to improve it.

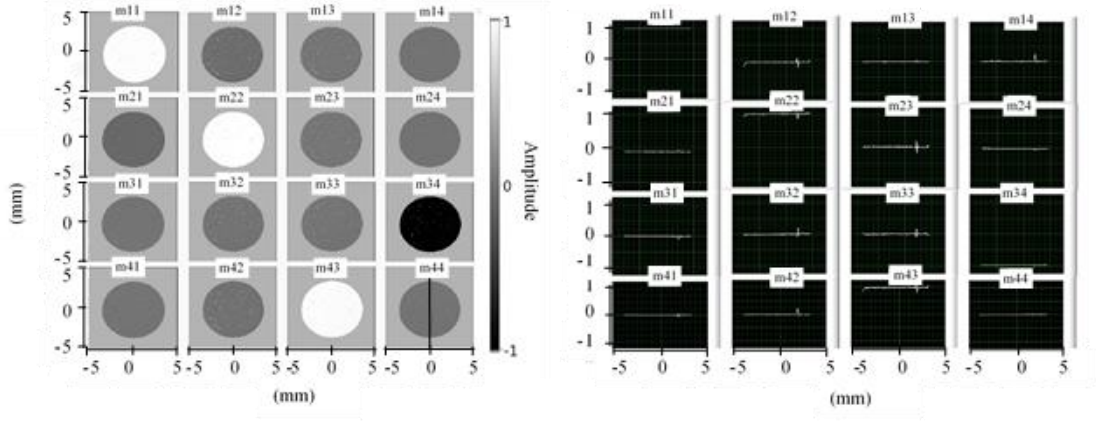


(a)The Mueller matrix image for QWP.

(b) Line profile of Mueller matrix along the central Y axis (Marked in image m44).

Figure 3.4. Experimental images obtained for a quarter waveplate (QWP) as a sample. The Mueller matrix imaging capability of the system, its line profile along the central Y axis has shown.

## 3.2.2. CONCLUSIONS

We presented a calibration for diattenuation error of dual rotating retarder Mueller matrix polarimeter. The main objective is to compensate the diattenuation error of the retarders. To apply this algorithm it is necessary to minimize the azimuthal error of the retarders as well as a polarizer. An increment of accuracy is obtained by the proposed method. By the moment our proposal is capable to retrieve the diattenuation parameters, but it needs to be complemented with the Goldstein-Chipman-algorithm.

## 3.3Implementation of retardance and diattenuation error

The basic concept of dual rotating retarder polarimeter is to produce different polarizing states of the input beam, by a fixed polarizer followed by a rotating retarder, while detecting the polarization states of the output beam by a rotating retarder followed by a fixed analyzer. Depending on the rotation ratio of speeds of the retarders of the PSA and PSG ratio of the retarders, the Mueller matrix information can be retrieved by the harmonics of the signal. In the case of 5:1, 12 harmonics are generated. By using Fourier analysis on the signal dependence by the rotation ratio, Mueller matrix information of the sample can be retrieved [1,2]. By considering non-ideal components, calibration procedures can be implemented by taking into account the output signal variation due to these characteristics. In our approach, linear diattenuation characteristics were added along with the retardation characteristic of the retarders used.

Considering the maximum and minimum intensity transmittance of the retarder as $T_{max}$ and $T_{min}$, the linear diattenuation parameter of the retarder can be defined as:

$$D = \frac{T_{max} - T_{min}}{T_{max} + T_{min}} \qquad 3.16$$

Therefore, the diattenuation property of retarders can be modeled as $T_{max}$ and $T_{min}$ in its corresponding Mueller matrix of each retarder.

According to the decomposition of Mueller matrix, any Mueller matrix of a non-depolarizing element can be decomposed in diattenuation and retardance Mueller matrix [6]. By considering retarder as a non-depolarizing element, it can be said that the product of retardance Mueller matrix ($M_R$) and diattenuation Muller matrix ($M_D$) will give the Mueller matrix of retarder ($M_{RD}$) which has both retardance and diattenuation. For simplicity here we have considered only linear retardance and linear diattenuation.

$$M_{RD}(\theta, \delta, T_{max}, T_{min}) = M_R M_D = M_D M_R \qquad 3.17$$

Therefore,

$$M_{RD} = \begin{bmatrix} \tau_1 & \tau_2\, C & \tau_2\, S & 0 \\ \tau_2\, C & \tau_1 C^2 + S^2 cos\delta\tau_3 & (\tau_1 - cos\delta\tau_3) S\, C & -S\, sin\delta\tau_3 \\ \tau_2 S & (\tau_1 - cos\delta\tau_3) S\, C & \tau_1\, S^2 + C^2 cos\delta\tau_3 & C\, sin\delta\tau_3 \\ 0 & S\, sin\delta\tau_3 & -C\, sin\delta\tau_3 & cos\delta\tau_3 \end{bmatrix} \quad 3.18$$

$$\tau_1 = T_{max} + T_{min}\tau_2 = T_{max} - T_{min}\tau_3 = 2\sqrt{T_{max}T_{min}}$$
$$C = cos2\theta S = sin2\theta$$

Where **(Here or where?)** δ and θ are considered to be the retardance and orientation of the fast axis. For simplicity on the calculation, the orientation of both retardance and the diattenuation are considered equal. The Mueller matrix of the retarder will now depend on not only on the orientation angle, but it will also depend on its retardance and diattenuation parameter.

The setup of the polarimeter considering the retarders containing retardance and diattenuation errors is presented in Fig. 3.5. Where the output Stokes vector is $\boldsymbol{S}_{out}$ and

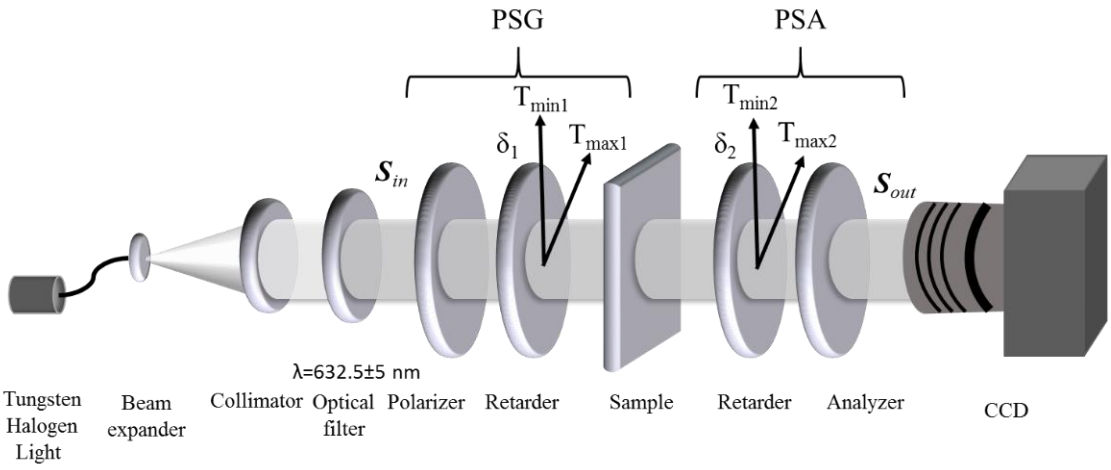


the input stokes vector is $\boldsymbol{S}_{in}$.

Figure 3.5 Dual rotating retarder polarimeter with diattenuation and retardation error of the retarder.

The output Stokes vector ($\boldsymbol{S}_{out}$) can be retrieved by multiplying the Mueller matrix of the elements with the input stokes vector ($\boldsymbol{S}_{in}$). The rotational angles of the PSG and PSA retarders are $\theta$ and $5\theta$. $M_{RD}$ carries the calibration parameters of the retarder that later will be retrieved. **(Space be given before $M_{RD}$)**

$$\begin{bmatrix} S_0 \\ S_1 \\ S_2 \\ S_3 \end{bmatrix}_{out} = \left[M_A\, M_{RD}\,(5\theta, \delta_2, T_{max2}, T_{min2}) M_S M_{RD}(\theta, \delta_1, T_{max1}, T_{min1}) M_p\right] \begin{bmatrix} S_0 \\ S_1 \\ S_2 \\ S_3 \end{bmatrix}_{in} \qquad 3.19$$

Where **(Here or Where?)** we consider the Mueller matrix of the PSA and PSG retarders as $M_{RD}(5\theta)$ and $M_{RD}(\theta)$ respectively, $M_s$ is the same of the sample under study and $M_p$ and $M_a$ as the analyzer and polarizer respectively. **(Space be given after $M_S$)**

$$M_S = \begin{bmatrix} m_{11} & m_{12} & m_{13} & m_{14} \\ m_{21} & m_{22} & m_{23} & m_{24} \\ m_{31} & m_{32} & m_{33} & m_{34} \\ m_{41} & m_{42} & m_{43} & m_{44} \end{bmatrix} \qquad 3.20$$

$M_S$ is considered to be the unknown Mueller matrix of the sample.

## 3.4Construction of Mueller matrix of the sample with errors compensation

By following the cascade matrix multiplication (Eq.3) of each Mueller matrix of the polarimeter, the output Stokes vector can be treated as a function of the Mueller matrix coefficients associated with the errors and the rotational angle of the retarders. As the errors of the retarders and the Mueller matrix coefficients are constants, therefore the output signal will vary only due to the rotation of the retarders. Hence the output signal will be periodic and it can be represented as a Fourier series. The Mueller matrix of the sample can be retrieved as the function of the complex Fourier coefficient of the output signal and the error parameters.

The first component of the output Stokes vector gives the output intensity of the output signal. So it is enough to consider only the first row of the PSA Mueller matrix and the Stokes vector of the light leaving the PSG optics [2]. This leads to the output signal as the sum of each Mueller matrix component multiplied with a coefficient:

$$S_{0\,out} = \sum_{i,j=1}^{4} \mu_{ij} m_{ij} \qquad 3.21$$

Where $S_{0\,out}$ is the first component of the output Stokes vector, the intensity information. $\mu_{ij}$ refers to the coefficient associated with the Mueller matrix components, $m_{ij}$, of the sample.

$$\mu_{11} = p_1p_2 + p_1q_2\,cos10\theta + q_1p_2cos2\theta + \frac{1}{2}q_1q_2(cos8\theta + cos12\theta)$$

$$\mu_{12} = \frac{1}{2}cos\delta_1p_2z_1m_{12} - \frac{1}{2}cos\delta_1p_2z_1cos4\theta + q_1p_2cos2\theta + \frac{1}{2}p_1p_2(1 + cos4\theta)$$
$$+ \quad \frac{1}{4}cos\delta_1q_2z_1(2cos10\theta - cos6\theta - cos14\theta) + \frac{1}{2}q_1q_2(cos8\theta + cos12\theta)$$
$$+ \frac{1}{4}p_1q_2(cos6\theta + \quad 2cos10\theta + cos14\theta)$$

$$\mu_{13} = q_1p_2sin2\theta + \frac{1}{2}p_2(p_1 - cos\delta_1z_1)sin4\theta + \frac{1}{2}q_1q_2(sin12\theta - sin8\theta)$$
$$+ \frac{1}{4}q_2(p_1 - \quad cos\delta_1z_1)(sin14\theta - sin6\theta)$$

$$\mu_{14} = sin\delta_1p_2z_1sin2\theta + \frac{1}{2}sin\delta_1q_2z_1(sin12\theta - sin8\theta)$$

$$\mu_{21} = p_1q_2\,cos10\theta + \frac{1}{2}p_1p_2(1 + cos20\theta) + \frac{1}{2}cos\delta_1p_1z_2(1 - cos20\theta)$$
$$+ \frac{1}{2}q_1q_2(cos8\theta + \quad cos12\theta) + \frac{1}{4}q_1p_2(2cos2\theta + cos18\theta\ + cos22\theta)$$
$$+ \frac{1}{4}cos\delta_2q_1z_2(2cos2\theta - cos18\theta - \quad cos22\theta)$$

$$\mu_{22} = \frac{1}{2}q_1q_2(cos8\theta + cos12\theta) + \frac{1}{4}p_1q_2(cos6\theta + 2cos10\theta + cos14\theta)$$

$$+ \quad \frac{1}{4}cos\delta_1q_2z_1(2cos10\theta - cos6\theta - cos14\theta)$$

$$+ \frac{1}{4}q_1p_2(2cos2\theta + cos18\theta + cos22\theta)$$

$$+ \quad \frac{1}{8}p_1p_2(2 + 2cos4\theta + cos16\theta + 2cos20\theta + cos24\theta)$$

$$+ \frac{1}{8}cos\delta_1p_2z_1(2 - 2cos4\theta - \quad cos16\theta + 2cos20\theta - cos24\theta)$$

$$+ \frac{1}{4}cos\delta_2q_1z_2(2cos2\theta - cos18\theta - cos22\theta)$$

$$+ \quad \frac{1}{8}cos\delta_2p_1z_2(2 + 2cos4\theta - cos16\theta - 2cos20\theta - cos24\theta)$$

$$+ \frac{1}{8}cos\delta_1cos\delta_2z_1z_2(2 - \quad 2cos4\theta + cos16\theta - 2cos20\theta + cos24\theta)$$

$$\mu_{23} = \frac{1}{2}q_1q_2(sin12\theta - sin8\theta) + \frac{1}{4}q_2(p_1 - cos\delta_1z_1)(sin14\theta - sin6\theta)$$

$$+ \frac{1}{4}q_1p_2(2sin2\theta - \quad sin18\theta + sin22\theta)$$

$$+ \frac{1}{8}p_2(p_1 - cos\delta_1z_1)(2sin4\theta - sin16\theta + sin24\theta)$$

$$+ \frac{1}{4}cos\delta_2p_1z_2(2sin2\theta + sin18\theta - sin22\theta) + \frac{1}{8}cos\delta_2z_2(p_1$$

$$- cos\delta_1z_1)(2sin4\theta + \quad sin16\theta - sin24\theta)$$

$$\mu_{24} = \frac{1}{2}sin\delta_1q_2z_1(sin12\theta - sin8\theta) + \frac{1}{4}sin\delta_1p_2z_1(2sin2\theta - sin18\theta - sin22\theta)$$

$$+ \quad \frac{1}{8}sin\delta_1cos\delta_2z_1z_2(2sin2\theta + sin18\theta - sin22\theta)$$

$$\mu_{31} = p_1q_2sin10\theta + \frac{1}{2}p_1(p_2 - cos\delta_2z_2)sin20\theta + \frac{1}{2}q_1q_2(sin12\theta + sin8\theta)$$

$$+ \frac{1}{4}q_1(p_2 - \quad cos\delta_2z_2)(sin18\theta + sin22\theta)$$

$$\mu_{32} = \frac{1}{2}q_1q_2(sin12\theta + sin8\theta) + \frac{1}{4}p_1q_2(sin6\theta + 2sin10\theta + sin14\theta)$$

$$+ \quad \frac{1}{4}cos\delta_1 q_2 z_1(2sin10\theta - sin6\theta + sin14\theta)$$

$$+ \frac{1}{4}q_1(p_2 - cos\delta_2 z_2)(sin18\theta + sin22\theta)$$

$$+ \quad \frac{1}{8}p_1(p_2 - cos\delta_2 z_2)(sin16\theta + 2sin20\theta + sin24\theta) + \frac{1}{8}cos\delta_1 z_1(p_2$$

$$- \quad cos\delta_2 z_2)(2sin20\theta - sin16\theta - sin24\theta)$$

$$\mu_{33} = \frac{1}{2}q_1q_2(cos8\theta - cos12\theta) + \frac{1}{4}q_2(p_1 - cos\delta_1 z_1)(cos6\theta - cos14\theta)$$

$$+ \frac{1}{4}q_1(p_2 - \quad cos\delta_2 z_2)(cos18\theta - cos22\theta)$$

$$+ \frac{1}{8}(p_1 - cos\delta_1 z_1)(p_2 - cos\delta_2 z_2)(cos16\theta - cos24\theta)$$

$$\mu_{34} = \frac{1}{2}sin\delta_1 q_2 z_1(cos8\theta - cos12\theta) + \frac{1}{4}sin\delta_1 z_1(p_2 - cos\delta_2 z_2)(cos18\theta - cos22\theta)$$

$$\mu_{41} = -sin\delta_2 p_1 z_2 sin10\theta - \frac{1}{2}sin\delta_2 q_1 z_2(sin12\theta + sin8\theta)$$

$$\mu_{42} = -\frac{1}{2}sin\delta_2 q_1 z_2(sin12\theta + sin8\theta) - \frac{1}{4}sin\delta_2 p_1 z_2(sin6\theta + 2sin10\theta + sin14\theta)$$

$$- \quad \frac{1}{4}cos\delta_1 sin\delta_2 z_1 z_2(2sin10\theta - sin6\theta + sin14\theta)$$

$$\mu_{43} = -\frac{1}{2}sin\delta_2 q_1 z_2(cos8\theta - cos12\theta) - \frac{1}{4}sin\delta_2 z_2(p_1 - cos\delta_1 z_1)(cos6\theta - cos14\theta)$$

$$\mu_{44} = -\frac{1}{2}sin\delta_1 sin\delta_2 z_1 z_2(cos8\theta - cos12\theta) \qquad 3.22$$

Where for convenience**,** some constants have been considered which contents the diattenuation and retardance error:

$$p_1 = T_{max1} + T_{min1}$$
$$q_1 = T_{max1} - T_{min1} \qquad 3.23$$

$$z_1 = 2\sqrt{T_{max1}T_{min1}}$$
$$p_2 = T_{max2} + T_{min2}$$
$$q_2 = T_{max2} - T_{min2}$$
$$z_2 = 2\sqrt{T_{max2}T_{min2}}$$
$$\beta_1 = p_1p_2 - p_2z_1cos\delta_1 - p_1z_2cos\delta_2 + cos\delta_1cos\delta_2z_1z_2$$
$$\beta_2 = p_1p_2 - p_2z_1cos\delta_1 + p_1z_2cos\delta_2 - cos\delta_1cos\delta_2z_1z_2$$
$$\beta_3 = p_1p_2 + p_2z_1cos\delta_1 - p_1z_2cos\delta_2 - cos\delta_1cos\delta_2z_1z_2$$
$$\beta_4 = p_1p_2 + p_2z_1cos\delta_1 + p_1z_2cos\delta_2 + cos\delta_1cos\delta_2z_1z_2$$
$$\alpha_1 = p_1p_2 - p_1z_2cos\delta_2$$
$$\alpha_2 = p_2p_1 - p_2z_1cos\delta_1$$
$$\alpha_3 = p_1p_2 + p_1z_2cos\delta_2$$
$$\alpha_4 = p_2p_1 + p_2z_1cos\delta_1$$

$\mu_{ij}$ depends on the rotational angle $\theta$, retardation and diattenuation of the two retarders. As the Mueller matrix coefficient and the retardation and diattenuation of the retarders are constants, the output intensity $S_{0\,out}$ will vary only for the rotational angle $\theta$.

Therefore, the output signal will be periodic and it can be represented as a Fourier series:

$$S_{0\,out} = a_0 + \sum_{n=1}^{12}\left(a_n\, cos2n\theta + \, b_n\, sin2n\theta\right) \qquad 3.24$$

Where $a_n$ and $b_n$ are the real and imaginary Fourier coefficients of the output signal. In this case, $a_n$ and $b_n$ are the function of retardance and diattenuation of the retarders and the Mueller matrix coefficient of the sample:

$$a_n, b_n \rightarrow f\left(m_{ij}, \delta_1, \delta_2, T_{max1}, T_{min1}, T_{max2}, T_{min2}\right) \quad 3.25$$

Where *f* refers to as function. As $a_n$ and $b_n$ do not depend on rotational angle $\theta$ or any other variable, the Mueller matrix elements of the sample $m_{ij}$ can be retrieved by the inverse calculation:

$$m_{11} = \frac{1}{p_1\, p_2 \alpha_1 \alpha_2 \beta_1}[\alpha_1\alpha_2\beta_1 a_0 - \alpha_1\alpha_4\beta_1 a_2 + (\alpha_1\alpha_4\beta_2 + \alpha_2\alpha_3\beta_3 - \alpha_1\alpha_2\beta_4)\, a_8 - \alpha_2\alpha_3\beta_1\, a_{10} + (\alpha_1\alpha_4\beta_2 + \alpha_3\beta_3 - \alpha_1\alpha_2\beta_4)\, a_{12}]$$

$$m_{12} = \frac{2}{\alpha_2\beta_1}(\beta_1 a_2 - \beta_2 a_8 - \beta_2 a_{12})$$

$$m_{13} = \frac{2}{\alpha_1\alpha_2}(\alpha_1 b_2 + \alpha_3 b_8 - \alpha_3 b_{12})$$

$$m_{14} = \frac{1}{sin\phi_1 p_2 z_1}\left(b_1 + \frac{2\alpha_3}{\alpha_1} b_9\right) - \frac{p_2 q_1}{sin\phi_1\, p_1\, p_2 \alpha_1 \alpha_2\, p_2 z_1}[2\, p_1\, p_2 \alpha_1 b_2 + (4\, p_1\, p_2 -)\alpha_3 b_8 + \alpha_2\alpha_3 b_{10} - \alpha_3\alpha_4 b_{12}]$$

$$m_{21} = \frac{2}{\alpha_1\beta_1}(\beta_1 a_{10} - \beta_3 a_8 - \beta_3 a_{12})$$

$$m_{22} = \frac{4}{\beta_1}(a_8 + a_{12})$$

$$m_{23} = \frac{4\, p_1 p_2}{\alpha_1\alpha_2}(b_{12} - b_8)$$

$$m_{24} = -\frac{4\, p_1\, p_2}{sin\phi_1 \alpha_1 p_2 z_1} b_9 + \frac{2\, p_2\, q_1}{sin\phi_1 \alpha_1 \alpha_2 p_2 z_1}[(4\, p_1\, p_2 - \alpha_4) b_8 + \alpha_2 b_{10} - \alpha_4 b_{12}]$$

$$m_{31} = \frac{2}{\alpha_1\alpha_2}(\alpha_2 b_{10} - \alpha_4 b_8 - \alpha_4 b_{12})$$

$$m_{32} = \frac{4\, p_1 p_2}{\alpha_1\alpha_2}(b_{12} + b_8)$$

$$m_{33} = \frac{4\, p_1 p_2}{\alpha_1\alpha_2}(a_8 - a_{12})$$

$$m_{34} = \frac{4\,p_1\,p_2}{sin\phi_1\alpha_1 p_2 z_1} a_9$$
$$- \frac{2\,p_2\,q_1}{sin\phi_1\alpha_1\alpha_2 p_2 z_1\beta_1}[(2\alpha_1\alpha_2 + 2\,p_1\,p_2\beta_1 - \alpha_2\beta_3)a_8 + \quad \alpha_2\beta_1\,a_{10}$$
$$- (2\,p_1\,p_2\beta_1 + \alpha_2\beta_3 - 2\alpha_1\alpha_2)a_{12}]$$
$$m_{41} = \frac{1}{sin\phi_2 p_1 z_2}\left(\frac{2\alpha_4}{\alpha_2} b_7 - b_5\right)$$
$$- \frac{p_1\,q_2}{sin\phi_2\,p_1\,p_2\alpha_1\alpha_2\,p_1 z_2}[\alpha_1\alpha_4 b_2 + \alpha_3\alpha_4 b_8 - \quad 2\,p_1 p_2\alpha_2 b_{10}$$
$$+ (4\,p_1 p_2 - \alpha_3)\alpha_4 b_{12}]$$
$$m_{42} = -\frac{4p_1\,p_2}{sin\phi_2\alpha_2\,p_1 z_2} b_7 + \frac{2\,p_1\,q_2}{sin\phi_2\alpha_1\alpha_2\,p_1 z_2}[\alpha_1 b_2 + \alpha_3 b_8 + (4\,p_1\,p_2 - \alpha_3)b_{12}]$$
$$m_{43} = \frac{4\,p_1 p_2}{sin\phi_2\alpha_2\,p_1 z_2} a_7$$
$$- \frac{2\,p_1 q_2}{sin\phi_2\alpha_1\alpha_2\,p_1 z_2\beta_1}[\alpha_1\beta_1\,a_2 \qquad 3.26$$
$$- (\alpha_1\beta_2 + 2\alpha_1\alpha_2 - \quad 2\,p_1\,p_2\beta_1)a_8 + (2\,p_1\,p_2\beta_1 + 2\alpha_1\alpha_2$$
$$- \alpha_1\beta_2)a_{12}]$$
$$m_{44} = \frac{1}{sin\phi_1 sin\phi_2 z_1 z_2}\left[(a_6 - a_4) + \frac{4\,p_1 q_2}{\alpha_1} a_9 - \frac{4\,q_1 p_2}{\alpha_2} a_7 + \frac{4\,p_1 p_2 q_1 q_2}{\alpha_1\alpha_2}(a_8 - \quad a_{12})\right.$$
$$+ \frac{2\,q_1 q_2}{\alpha_1\alpha_2\beta_1}[\alpha_1\beta_1\,a_2 - (\alpha_1\beta_2 + 4\alpha_1\alpha_2 - \alpha_2\beta_3)a_8 - \alpha_2\beta_1\,a_{10}$$
$$\left. + \quad (4\,p_1\,p_2\beta_1 + \alpha_2\beta_3 - \alpha_1\beta_2)a_{12}]\right]$$

The normalization of the Mueller matrix component can be done by dividing all $m_{ij}$ by $m_{11}$.

In order to calculate the Mueller matrix element of an unknown sample by the proposed equations, it is necessary to retrieve the value of the error constants. The no-sample calibration method is used to retrieve the error constants of the retarders.

## 3.5Error calibration by taking non-sample approach

For calibration of the error due to the imperfect retarder**,** it is necessary to know the true value of retardance and diattenuation of the retarders. The calibration algorithm for the errors as described in this section to implement the approached model has been described in the last section.

An experiment without any sample has been done in order to retrieve the value of the error constants (shown in Eq.9). In this case**,** the Mueller matrix will be identical:

$$M_S = \begin{bmatrix} 1 & 0 & 0 & 0 \\ 0 & 1 & 0 & 0 \\ 0 & 0 & 1 & 0 \\ 0 & 0 & 0 & 1 \end{bmatrix}_{No\ sample} \qquad 3.27$$

Therefore, according to Eq.5, the Stokes vector of the output signal will contain only four coefficient ($\mu_{ij}$) associate with the Mueller matrix components. Here also $\mu_{ij}$ depends on the rotational angle $\theta$, retardation and diattenuation of the two retarders. But unlike the previous case**,** the output intensity ($S_{0\,out}$) will not depend on Mueller matrix element of the sample ($m_{ij}$), it will depend on the retardance and diattenuation of the retarders and the rotational angle.

Therefore, the complex Fourier components of the output signal also will not depend on the Mueller matrix elements ($m_{ij}$), it will depend on the error constants only, i.e. they will be a function of retardation and diattenuation of the retarders.

As in this case, the complex Fourier components depend on retardation and diattenuation only, so the error constants can be retrieved by the inverse calculation of the complex Fourier coefficients.

The diattenuation of the retarders will be:

$$D_1 = \frac{T_{max1} - T_{min1}}{T_{max1} + T_{min1}} = \frac{q_1 p_2}{p_1 p_2} = \frac{a_1 + a_9}{a_0 + a_2 + a_8 + a_{10}}$$

$$D_2 = \frac{T_{max2} - T_{min2}}{T_{max2} + T_{min2}} = \frac{p_1 q_2}{p_1 p_2} = \frac{a_3 + a_5}{a_0 + a_2 + a_8 + a_{10}} \qquad 3.28$$

The retardance of the retarders will be:

$$\delta_1 = \cos^{-1}\left[\frac{2\,(a_0 - 3\,a_2 - 3\,a_8 + a_{10})}{\sqrt{c_1 - c_2}}\right]$$

$$\delta_2 = \cos^{-1}\left[\frac{2\,(a_0 + \,a_2 - 3\,a_8 - 3\,a_{10})}{\sqrt{c_1 - c_3}}\right] \qquad 3.29$$

Where:

$$\begin{aligned} c_1 = {} & 4{a_0}^2 + 8a_0a_2 + 8a_0a_8 + 8a_0a_{10} + 4a_0a_4 + 4a_0a_6 + 4{a_2}^2 \\ & + \quad 8a_2a_8 + 8a_2a_{10} + 4a_2a_4 + 4a_2a_6 + 4\,{a_8}^2 + 8a_8a_{10} \\ & + 4a_4a_8 + \quad 4a_6a_8 + 4\,{a_{10}}^2 + 4a_4a_{10} + 4a_6a_{10} \\ c_2 = {} & 4\,{a_1}^2 + 8a_1a_9 + 4a_1a_3 + 4a_1a_5 + 4\,{a_9}^2 + 4a_3a_9 + 4a_5a_9 \\ c_3 = {} & 4a_1a_3 + 4a_1a_5 + 4a_3a_9 + 4a_5a_9 + 4\,{a_3}^2 + 8a_3a_5 + 4\,{a_5}^2 \end{aligned} \qquad 3.30$$

And the error constants will be:

$$\begin{aligned} p_1p_2 &= \frac{1}{2}\,(a_0 + a_2 + a_8 + a_{10}) \\ q_1q_2 &= \frac{1}{2}\,(a_4 + a_6) \\ q_1p_2 &= \frac{1}{2}\,(a_1 + a_9) \\ p_1q_2 &= \frac{1}{2}\,(a_3 + a_5) \\ z_1z_2 &= \frac{1}{2}\,[(a_0 + a_2 + a_4 + a_6 + a_8 + a_{10}) - (a_1 + a_3 + a_5 + a_9)^2]^{1/2} \end{aligned} \qquad 3.31$$

$$p_2 z_1 = \frac{1}{4}\sqrt{c_1 - c_2}$$

$$p_1 z_2 = \frac{1}{4}\sqrt{c_1 - c_3}$$

Where $c_1$, $c_2$, $c_3$ are same as Eq.3.30.

Now, this value should be substituted back in Eq.3.26 to calculate the Mueller matrix of any sample.

## 3.6Experimental results

The Mueller matrix polarimeter consists of a tungsten halogen light source, a narrow band-pass filter of wavelength 632.5±5 nm, Glan-Thompson polarizers and zero- order quartz quarter waveplate at 632.5 nm. A 14 bit CCD camera (Thorlab-8050M-GE-TE) was used to capture 36 images over a rotating of 180$^{o}$ (36×5 $^{o}$) of the first retarder. In each position**,** 20 images were taken and averaged in order to reduce noise.

The algorithm is based on the Azzam's model of dual rotating retarder polarimeter [1]. The effect of diattenuation and retardation error has implemented in this model. The calibration of the Goldstein-Chipman algorithm also based on the Azzam's model [16]. Hence, the experimental results have compared only with the Azzam's algorithm and the Goldstein-Chipman algorithm to show the enhancement of accuracy by the proposed algorithm. There are also many other algorithms [16-21] to compensate errors of this polarimeter. But our proposed algorithm is the unique one which compensates the diattenuation error along with the retardation error.

The experimental results for no-sample and retarders are presented in two sections.

### 3.6.1 No-sample

The experimental results for no-sample are presented in Table 1; and have been compared with the - without calibration result, the Goldstein-Chipman algorithm results and theoretical value. In the table, the sum of the square of errors for all Mueller matrix elements has been shown and compared with an aim to measure the accuracy of each method. The numerical value is the value of one point of the image.

**Table 3.2 Experimental result for no sample**

| | Mueller matrix | Sum of square of errors for all elements | Theoretical value |
|---|---|---|---|
| Without calibration | $\begin{pmatrix} 1.000 & -0.023 & -0.009 & 0.003 \\ 0.046 & 0.937 & -0.022 & 0.006 \\ -0.019 & 0.030 & 0.952 & 0.003 \\ 0.004 & -0.001 & -0.049 & 0.982 \end{pmatrix}$ | 0.013 | |
| Goldstein-Chipman algorithm | $\begin{pmatrix} 1.000 & 0.004 & -0.016 & 0.003 \\ 0.004 & 0.950 & 0.033 & 0.006 \\ -0.002 & -0.025 & 0.965 & 0.003 \\ -0.002 & 0.009 & -0.051 & 0.983 \end{pmatrix}$ | 0.009 | $\begin{pmatrix} 1 & 0 & 0 & 0 \\ 0 & 1 & 0 & 0 \\ 0 & 0 & 1 & 0 \\ 0 & 0 & 0 & 1 \end{pmatrix}$ |
| Proposed algorithm | $\begin{pmatrix} 1.000 & -0.019 & -0.010 & -0.001 \\ -0.018 & 0.994 & -0.024 & 0.013 \\ -0.021 & 0.032 & 1.010 & 0.021 \\ 0.011 & -0.014 & -0.011 & 0.984 \end{pmatrix}$ | 0.004 | |

In the results shown in the Table 3.2, all Mueller matrix elements are normalized by $m_{11}$. For $m_{22}$ and $m_{33}$ where the theoretical value is 1, the error obtained by the proposed algorithm is 1% whereas by other methods it is about 5%. In the case of m44, the error is about 2% obtained by all processes. For $m_{43}$, the error is nearly 1% by the proposed algorithm whereas by other methods it is about 5%. For $m_{23}$ the error is about 2-3% for every method. For all other elements, 1-2% errors have been obtained.

In the case of the sum of the square of errors, the error of each element has been squared and added. It clearly reflects the overall error obtained by each method. For the other methods, it is nearly or more than 0.01 but for the proposed method it is 0.004.

The image of the Mueller matrix for no sample obtained by the proposed algorithm has shown in Fig.2 in order to show the variation over space. The line profile has also been shown in order to show the one-dimensional variation. The line, whose profile has been drawn, has mentioned in the image of $m_{44}$.

### 3.6.2 Retarder analysis variation using QWP and Babinet-Soleil compensator

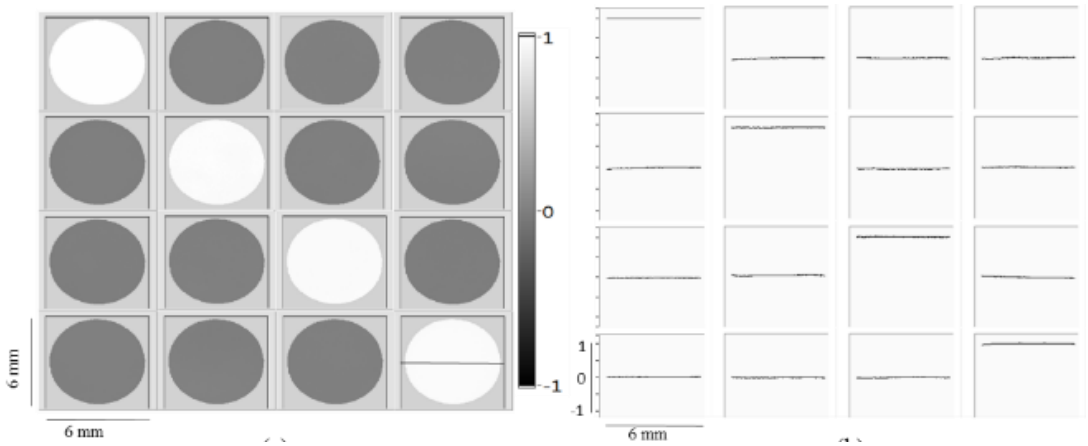


Figure 3.6 (a) 2-dimensional plot of Mueller matrix for no-sample. (b) 1-dimensional line profile along horizontal axis.

The experiment has been carried out taking a QWP and a variable retarder (Soleil-Babinet compensator) as a sample. The retardance of the sample can be obtained after decomposing the Mueller matrix [6,7]. To measure the retardance of the sample is one of the challenging jobs in polarimetry. High accuracy of the system is needed to measure the retardance accurately since small errors in the system may change the result significantly.

The decomposed image of retardance of the sample (QWP) is presented without calibration and after calibration of diattenuation and retardation error (Fig.3.7). The variation of retardance of the QWP is much more in the case of without calibration results than after calibration results. Although little fluctuations can be observed, yet stability in the overall nature also can be observed in the case of calibrated results. On the other hand, in the case of without calibration result, there is a possibility for occurrence of fluctuation of retardance over space.

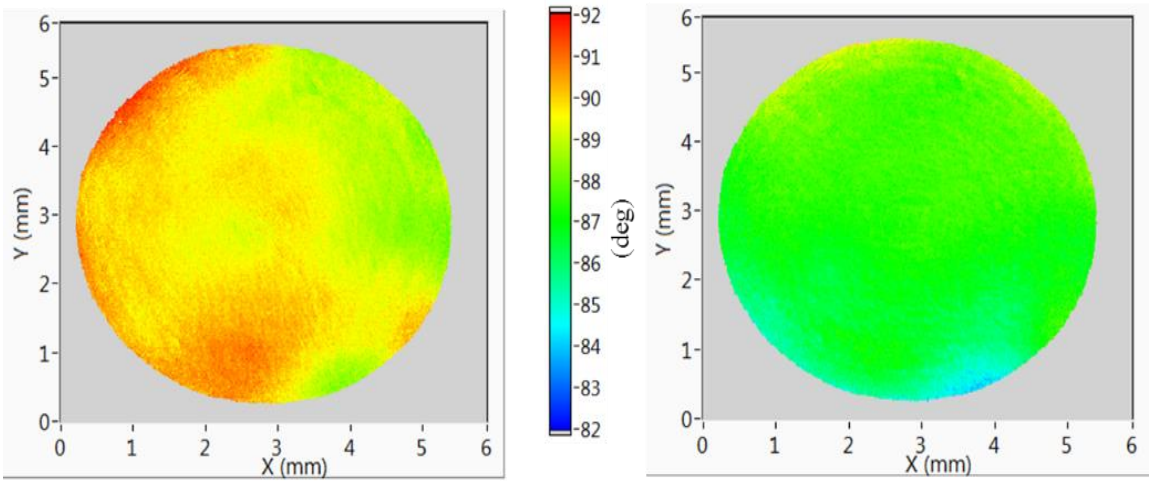


Figure 3.7 Fig. The retardance of a QWP obtained by decomposing its Mueller matrix. (a) is the 2-dimensional plot of retardance of a retarders as a sample obtained without calibration. (b) is the same obtained after calibration by proposed algorithm.

Babinet-Soleil Compensator is a variable retarder constructed by 2 wedge quartz crystals. The retardance of the system changes linearly concerning the movement of one quartz plate. The experiment results for a Babinet-Soleil Compensatoris shown in Fig.3.58. The retardance has been calculated by decomposing the Mueller matrix over displacement.

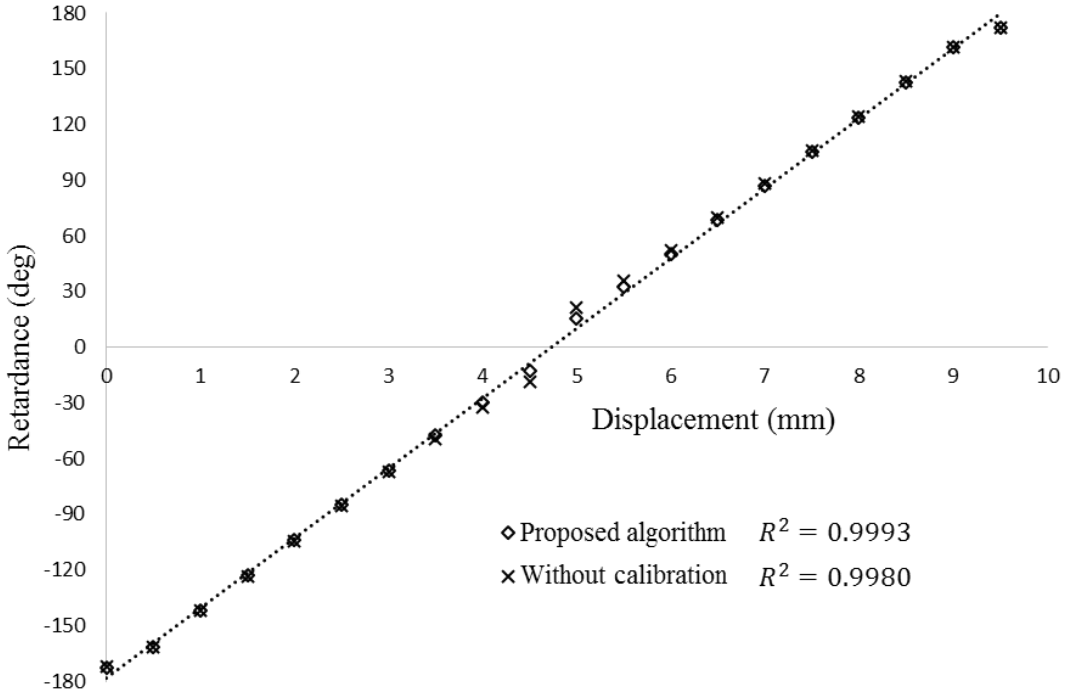


Figure 3.8 The variation of retardance of a Babinet-Soleil Compensator over displacement.

Fig.3.5 shows variation of retardance over displacement which is obtained at a point of the CCD camera. An arccos function has been used to determine the value of retardance as per the Lu-Chipman Mueller matrix decomposition method [6]. The results are limited between 0º to 180º, so it has been unwrapped intend to get the variation from -180 º to 180º. Both results obtained by the proposed algorithm and without calibration method have been shown. The dotted line indicates the linear

trendline. The trendline for both results became the same. As expected, the obtained values are linear, which supports the theoretical phenomena of Babinet-Soleil Compensator. The coefficient of determination ($R^2$) values has also been shown to measure the linearity of the obtained data. Here also the data obtained by the proposed method is more linear than without the calibration method.

# 4 Enhancement in time of Mueller matrix polarimeter

To do enhancement in time of Mueller matrix polarimeter, our proposal is to construct a single shot Mueller matrix polarimeter using the property of channelled spectrum and axially symmetric quarter waveplate [23][24]. A circular grating has used here instead of conventional grating. The proposed set up has described with a supporting algorithm.

Mueller matrix polarimeter is constructed by modulating the polarizing state of the input beam in polarizing state generator and also analysing the polarizing state of the output beam in polarizing state analyser. This modulation is generally done by modulation in the time domain [1], modulation in the spatial domain [24], modulation in spectral domain [23]. But to construct a single shot Mueller matrix polarimeter using this kind of modulation is a little difficult.

Here we have proposed to construct a single shot Mueller matrix polarimeter using the combination of spatial domain modulation and spectral domain modulation of polarization.

For spatial domain modulation of polarization, an achromatic axially symmetric wave plate (AASWP) has been used [24]. Achromatic axially symmetric wave plate (AASWP) acts like a Fresnel rhomb and introduce phase difference between the two axes of the beam. So that it behaves like a retarder where retardance remains constant but the fast axis orientation varies over the space.

For spectral domain modulation, the theory of channelled spectrum has been adopted [23] and thus two high order retarders and a polarizer have been used. When broadband wavelength light passes through high order retarders, the retarders introduce different phase for each wavelength. By using a grating, these wavelengths can be separated and modulation over the space can be measured.

For the grating**,** a circular or radial grating has been used. This is a tricky thing for this proposal. Generally, gratings are linear or crossed, but here circular grating is used to separate the wavelengths radially.

## 4.1 Proposed setup

In the proposed arrangement as shown in Fig.4.1, the PSG consists of a broadband light source followed by a polarizer with its transmission axis at $0^o$ and two thick retarders with directions and magnitudes of retardance $45^o$, $\delta_1$ and $0^o$, $\delta_2$ respectively. Where $\delta_1$ and $\delta_2$ are functions of wavenumber k. The PSA consists of and an achromatic axially symmetric quarter waveplate (AASQWP) and an analyser oriented at 0°. The channelled spectra are generated by diffraction from a circular grating and the spatio-spectrally signal is collected through a lens and recorded on the CCD.

Achromatic axially symmetric quarter waveplate (AASQWP) and an analyser oriented at 0◦ has been used as polarizing state analyser (PSA); and a polarizer and two high order retarder oriented at $0^o$,$45^o$ and $0^o$ has been used as polarizing state generator (PSG) [Fig:4.1].

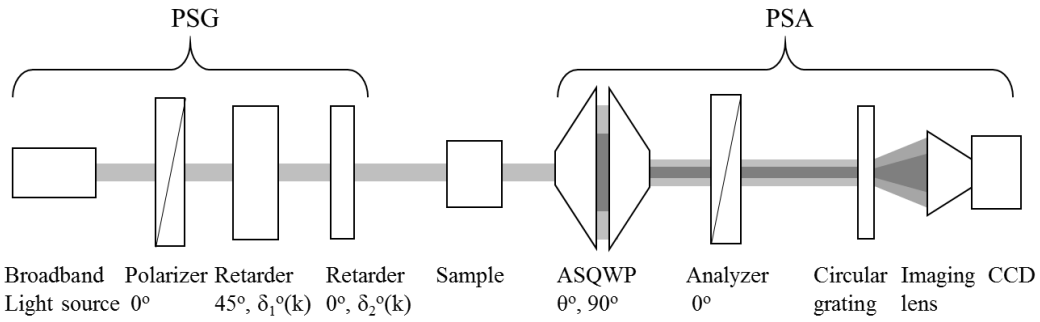


Fig. 4.1 Experimental setup for single shot Mueller matrix polarimeter

A white light source has been used followed by a collimating lens. A circular grating has been used to separate the wavelengths radially. A lens system and CCD has been used to capture the image.

## 4.2 Theory

According to the theory of Mueller matrix, the output Stokes vector can be written as

$$S_{out}(k) = M_A \; M_{ASQWP} \; M_S \; M_{R2(k)} \; M_{R1(k)} \; S_{in} \tag{4.1}$$

Where 'k' denotes the wave number which is the reciprocal of the wavelength. 'M' denotes the Mueller matrix of each component.

The output intensity will be

$$S_{out}(k) = \begin{bmatrix} 1 & 1 & 0 & 0 \\ 1 & 1 & 0 & 0 \\ 0 & 0 & 0 & 0 \\ 0 & 0 & 0 & 0 \end{bmatrix} \begin{bmatrix} 1 & 0 & 0 & 0 \\ 0 & \cos^2 2\theta & sin2\theta cos2\theta & -sin2\theta \\ 0 & sin2\theta cos2\theta & \sin^2 2\theta & cos2\theta \\ 0 & sin2\theta & -cos2\theta & 0 \end{bmatrix} \begin{bmatrix} m_{11} & m_{12} & m_{13} & m_{14} \\ m_{21} & m_{22} & m_{23} & m_{24} \\ m_{31} & m_{32} & m_{33} & m_{34} \\ m_{41} & m_{42} & m_{43} & m_{44} \end{bmatrix}$$
$$\times \begin{bmatrix} 1 & 0 & 0 & 0 \\ 0 & 1 & 0 & 0 \\ 0 & 0 & cos\delta_2(k) & sin\delta_2(k) \\ 0 & 0 & -sin\delta_2(k) & cos\delta_2(k) \end{bmatrix} \begin{bmatrix} 1 & 0 & 0 & 0 \\ 0 & cos\delta_1(k) & 0 & -sin\delta_1(k) \\ 0 & 0 & 1 & 0 \\ 0 & sin\delta_1(k) & 0 & cos\delta_1(k) \end{bmatrix} \begin{bmatrix} 1 \\ 1 \\ 0 \\ 0 \end{bmatrix} \tag{4.2}$$

From this equation, the output intensityor the 1st component of the output Stokes vector can be calculated by matrix multiplication method.

$$\begin{aligned} S_{0_{out}}(k) = & \left( m_{11} + \cos^2 2\theta \, m_{21} + \frac{1}{2} sin4\theta m_{31} - sin2\theta m_{41} \right) \\ & + \left( m_{12} + \cos^2 2\theta \, m_{22} + \frac{1}{2} sin4\theta m_{32} - sin2\theta m_{42} \right) cos\delta_1(k) \\ & + \left( m_{13} + \cos^2 2\theta \, m_{23} + \frac{1}{2} sin4\theta \, m_{33} - sin2\theta \, m_{43} \right) sin\delta_1(k) sin\delta_2(k) \\ & + \left( m_{14} + \cos^2 2\theta \, m_{24} + \frac{1}{2} sin4\theta m_{34} - sin2\theta m_{44} \right) sin\delta_1(k) cos\delta_2(k) \end{aligned} \tag{4.3}$$

Where $\delta_1(k)$ and $\delta_2(k)$ are the retardance of two retarders, k is wave number and $\theta$ is the orientation of azimuthal angle of the AASQWP.

In the image, there will be spatial variation both for channeled spectrum and ASQWP. If we take a circular line, there will be variation for azimuthal angle ($\theta$) of the ASQWP but there will be no variation for wavenumber ($k$) (as circular grating has used). Similarly, if we take a straight line through the center, there will be spatial variation for wavenumber ($k$) but there will be no variation for azimuthal angle ($\theta$) of the ASQWP.

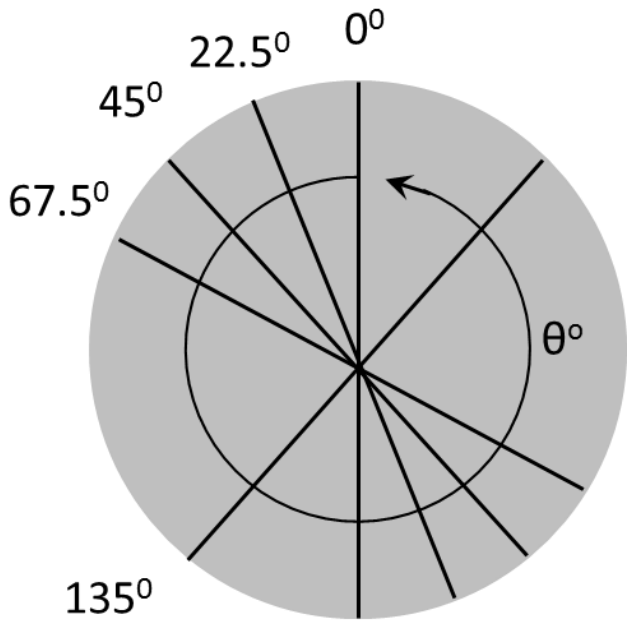


Fig. 4.2 Output image

So here we take some line at θ=0º, 22.5º, 45º, 67.5º, 135º; the intensity distribution along these lines will be different due to the modulation of AASQWP and we will get different intensity distribution. The intensity distribution of each line can be denoted as $I_N(k)$.

**At θ=0°,**

$$I_1(k) = \left(m_{11} + 1m_{21} + \frac{1}{2}\,0\,m_{31} - 0m_{41}\right) + \left(m_{12} + 1m_{22} + \frac{1}{2}\,0m_{32} - 0m_{42}\right) cos\delta_1(k) + \left(m_{13} + 1m_{23} + \frac{1}{2}0m_{33} - 0m_{43}\right) sin\delta_1(k) sin\delta_2(k) + \left(m_{14} + 1m_{24} + \frac{1}{2}0m_{34} - 0m_{44}\right) sin\delta_1(k) cos\delta_2(k) \quad 4.4$$

**At θ=22.5°,**

$$I_2(k) = \left(m_{11} + \frac{1}{2}m_{21} + \frac{1}{2}m_{31} - \frac{1}{\sqrt{2}}m_{41}\right) + \left(m_{12} + \frac{1}{2}m_{22} + \frac{1}{2}m_{32} - \frac{1}{\sqrt{2}}m_{42}\right) cos\delta_1(k) + \left(m_{13} + \frac{1}{2}m_{23} + \frac{1}{2}m_{33} - \frac{1}{\sqrt{2}}m_{43}\right) sin\delta_1(k) sin\delta_2(k) + \left(m_{14} + \frac{1}{2}m_{24} + \frac{1}{2}m_{34} - \frac{1}{\sqrt{2}}m_{44}\right) sin\delta_1(k) cos\delta_2(k) \quad 4.5$$

**At θ=45°,**

$$I_3(k) = \left(m_{11} + 0m_{21} + \frac{1}{2}\,0\,m_{31} - 1m_{41}\right) + \left(m_{12} + 0\,m_{22} + \frac{1}{2}\,0m_{32} - 1m_{42}\right) cos\delta_1(k) + \left(m_{13} + 0m_{23} + \frac{1}{2}0m_{33} - 1m_{43}\right) sin\delta_1(k) sin\delta_2(k) + \left(m_{14} + 0m_{24} + \frac{1}{2}0m_{34} - 1m_{44}\right) sin\delta_1(k) cos\delta_2(k) \quad 4.6$$

**At θ=67.5°,**

$$I_4(k) = \left(m_{11} + \frac{1}{2}m_{21} - \frac{1}{2}m_{31} - \frac{1}{\sqrt{2}}m_{41}\right) + \left(m_{12} + \frac{1}{2}m_{22} - \frac{1}{2}m_{32} - \frac{1}{\sqrt{2}}m_{42}\right) cos\delta_1(k) + \left(m_{13} + \frac{1}{2}m_{23} - \frac{1}{2}m_{33} - \frac{1}{\sqrt{2}}m_{43}\right) sin\delta_1(k)sin\delta_2(k) + \left(m_{14} + \frac{1}{2}m_{24} - \frac{1}{2}m_{34} - \frac{1}{\sqrt{2}}m_{44}\right) sin\delta_1(k)cos\delta_2(k) \quad 4.7$$

**At θ=135°,**

$$I_5(k) = \left(m_{11} + 0m_{21} + \frac{1}{2}\,0\,m_{31} + 1m_{41}\right) + \left(m_{12} + 0\,m_{22} + \frac{1}{2}\,0m_{32} + 1m_{42}\right) cos\delta_1(k) + \left(m_{13} + 0m_{23} + \frac{1}{2}0m_{33} + 1m_{43}\right) sin\delta_1(k)sin\delta_2(k) + \left(m_{14} + 0m_{24} + \frac{1}{2}0m_{34} + 1m_{44}\right) sin\delta_1(k)cos\delta_2(k) \quad 4.8$$

By some algebraic calculation we can get:

$$\frac{1}{2}(I_3(k) + I_5(k)) = m_{11} + m_{12}\,cos\delta_1(k) + m_{13}\,sin\delta_1(k)sin\delta_2(k) + m_{14}sin\delta_1(k)cos\delta_2(k)$$

$$I_1 - \frac{1}{2}(I_3(k) + I_5(k)) = m_{21} + m_{22}\,cos\delta_1(k) + m_{23}\,sin\delta_1(k)sin\delta_2(k) + m_{24}sin\delta_1(k)cos\delta_2(k)$$

$$(I_2(k) - I_4(k)) = m_{31} + m_{32}\,cos\delta_1(k) + m_{33}\,sin\delta_1(k)sin\delta_2(k) + m_{34}sin\delta_1(k)cos\delta_2(k) \quad 4.9$$

$$\frac{1}{2}(I_5(k) - I_3(k)) = m_{41} + m_{42}\,cos\delta_1(k) + m_{43}\,sin\delta_1(k)sin\delta_2(k) + m_{44}sin\delta_1(k)cos\delta_2(k)$$

Now, by FFT we can get all Mueller matrixes.

**From** $\frac{1}{2}(\boldsymbol{I_3(k)} + \boldsymbol{I_5(k)})$ **:**

$$\frac{1}{2}(I_3(k) + I_5(k)) = m_{11} + m_{12}\, cos\delta_1(k) + m_{13}\, sin\delta_1(k) sin\delta_2(k) + m_{14} sin\delta_1(k) cos\delta_2(k)$$

$$\Rightarrow \frac{1}{2}(I_2(k) + I_5(k)) = m_{11} + m_{12}\, cos\delta_1(k) + m_{13}\frac{1}{2}\{\cos(\delta_1(k) - \delta_2(k)) - \cos(\delta_1(k) + \delta_2(k))\} + m_{14}\frac{1}{2}\{\sin(\delta_1(k) - \delta_2(k)) + \sin(\delta_1(k) + \delta_2(k))\} \quad 4.10$$

The simulation of output Intensity Distribution is shown in Fig 4.3:

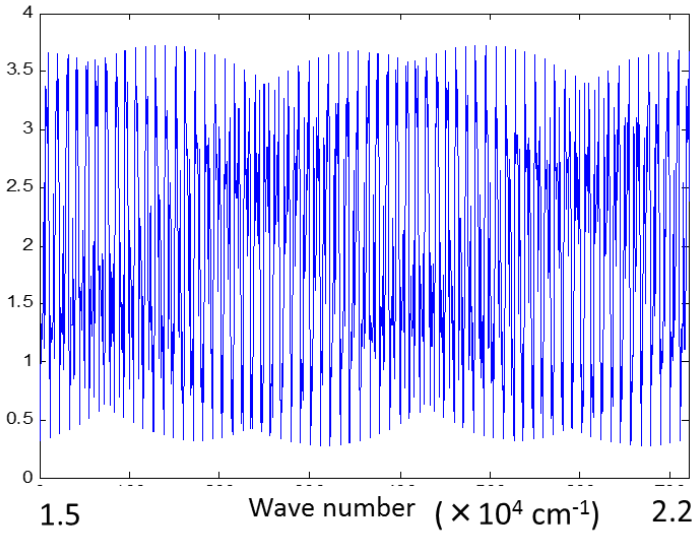


Figure 4.3 Output Intensity Distribution

By Fast Fourier transform we can obtain the Fourier coefficient.

$$a_{10} = m_{11}$$
$$a_{11} = m_{12}$$
$$a_{1-} = \frac{1}{2} m_{13}$$
$$a_{1+} = -\frac{1}{2} m_{13} \qquad 4.11$$
$$b_{1-} = \frac{1}{2} m_{14}$$
$$b_{1+} = \frac{1}{2} m_{14}$$

Therefore, the 4 Mueller matrix component of the sample can be obtained in terms of the Fourier coefficient.

$$m_{11} = a_{10}$$
$$m_{12} = a_{11}$$
$$m_{13} = 2a_{1-} = -2a_{1+} \qquad 4.12$$
$$m_{14} = 2b_{1-} = 2b_{1+}$$

As these are obtained from the 1st set of the equation, suffix 1 is added with all Fourier coefficients.

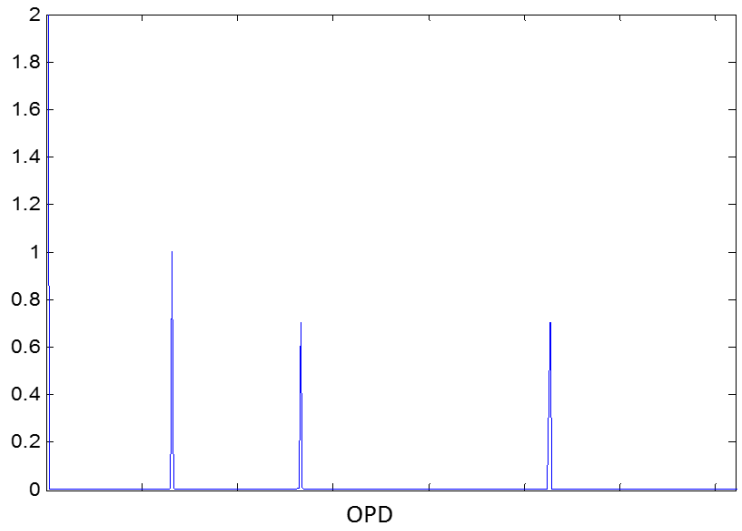


Figure 4.4 FFT plot of channeled spectrum

Similarly, **from** $\boldsymbol{I_1(k) - \frac{1}{2}(I_2(k) + I_5(k))}$ **:**

$$I_1(k) - \frac{1}{2}(I_2(k) + I_5(k)) = m_{21} + m_{22}\, cos\delta_1(k) + m_{23} sin\delta_1(k) sin\delta_2(k) + m_{24} sin\delta_1(k) cos\delta_2(k)$$

$$\Rightarrow I_1(k) - \frac{1}{2}(I_2(k) + I_5(k)) = m_{21} + m_{22}\, cos\delta_1(k) + m_{23}\frac{1}{2}\{\cos(\delta_1(k) - \delta_2(k)) - \cos(\delta_1(k) + \delta_2(k))\} + m_{24}\frac{1}{2}\{\sin(\delta_1(k) - \delta_2(k)) + \sin(\delta_1(k) + \delta_2(k))\} \quad 4.13$$

By Fast Fourier transform, we can obtain the Fourier coefficient.

$$a_{20} = m_{21}$$

$$a_{21} = m_{22}$$

$$a_{2-} = \frac{1}{2}m_{23}$$

$$a_{2+} = -\frac{1}{2}m_{23} \quad 4.14$$

$$b_{2-} = \frac{1}{2}m_{24}$$

$$b_{2+} = \frac{1}{2}m_{24}$$

Therefore, the 4 Mueller matrix component of the sample can be obtained in terms of Fourier coefficient.

$$m_{21} = a_{20}$$

$$m_{22} = a_{21}$$

$$m_{23} = 2a_{2-} = 2a_{2+} \qquad 4.15$$

$$m_{24} = 2b_{2-} = 2b_{2+}$$

As these are obtained from 2nd set of equation, so suffix 1 is added with all Fourier coefficients.

Similarly, **from** $(\boldsymbol{I_2(k) - I_4(k)})$ **:**

$$\frac{1}{2}(I_2(k) + I_5(k)) = m_{31} + m_{32}\, cos\delta_1(k) + m_{33} sin\delta_1(k) sin\delta_2(k) + m_{34} sin\delta_1(k) cos\delta_2(k)$$

$$\Rightarrow \frac{1}{2}(I_2(k) + I_5(k)) = m_{31} + m_{32}\, cos\delta_1(k) + m_{33}\frac{1}{2}\{\cos(\delta_1(k) - \delta_2(k)) - \cos(\delta_1(k) + \delta_2(k))\} + m_{34}\frac{1}{2}\{\sin(\delta_1(k) - \delta_2(k)) + \sin(\delta_1(k) + \delta_2(k))\} \qquad 4.16$$

By Fast Fourier transform, we can obtain the Fourier coefficient.

$$a_{30} = m_{31}$$

$$a_{31} = m_{32}$$

$$a_{3-} = \frac{1}{2}m_{33} \qquad 4.17$$

$$a_{3+} = -\frac{1}{2}m_{33}$$

$$b_{3-} = \frac{1}{2} m_{34}$$

$$b_{3+} = \frac{1}{2} m_{34}$$

Therefore, the 4 Mueller matrix component of the sample can be obtained in terms of the Fourier coefficient.

$$\begin{aligned} m_{31} &= a_{30} \\ m_{32} &= a_{31} \\ m_{33} &= 2a_{3-} = -2a_{3+} \end{aligned} \qquad 4.18$$

$$m_{34} = 2b_{3-} = 2b_{3+}$$

As these are obtained from the 3rd set of the equation, suffix 1 is added with all Fourier coefficients.

Similarly, **from** $\frac{1}{2}(\boldsymbol{I_5(k) - I_3(k)})$**:**

$$\begin{aligned} &\frac{1}{2}(I_5(k) - I_3(k)) \\ &\quad = m_{41} + m_{42}\, cos\delta_1(k) + m_{43} sin\delta_1(k) sin\delta_2(k) \\ &\quad + \quad m_{44} sin\delta_1(k) cos\delta_2(k) \end{aligned}$$

$$\begin{aligned} \Rightarrow &\frac{1}{2}(I_5(k) - I_3(k)) \\ &= m_{41} + m_{42}\, cos\delta_1(k) \\ &+ m_{43}\frac{1}{2}\{\cos(\delta_1(k) - \delta_2(k)) - \cos(\delta_1(k) + \delta_2(k))\} \\ &+ m_{44}\frac{1}{2}\{\sin(\delta_1(k) - \delta_2(k)) + \sin(\delta_1(k) + \delta_2(k))\} \end{aligned} \qquad 4.19$$

By Fast Fourier transform**,** we can obtain the Fourier coefficient.

$$a_{40} = m_{41} \qquad 4.20$$

$$a_{41} = m_{42}$$

$$a_{4-} = \frac{1}{2} m_{43}$$

$$a_{4+} = -\frac{1}{2} m_{43}$$

$$b_{4-} = \frac{1}{2} m_{44}$$

$$b_{4+} = \frac{1}{2} m_{44}$$

Therefore, the 4 Mueller matrix component of the sample can be obtained in terms of Fourier coefficient.

$$m_{41} = a_{40}$$

$$m_{42} = a_{41}$$

$$m_{43} = 2a_{4-} = -2a_{4+} \qquad 4.21$$

$$m_{44} = 2b_{4-} = 2b_{4+}$$

As these are obtained from the 4th set of the equation, suffix 1 is added with all Fourier coefficients.

So finally we can write the equation of all Muller matrix coefficients together as:

**Table 4.1. Equation of Mueller matrix elements of the sample**

| | | | |
|---|---|---|---|
| $\boldsymbol{m_{11} = a_{10}}$ | $\boldsymbol{m_{12} = a_{11}}$ | $\boldsymbol{m_{13} = 2a_{1-} = -2a_{1+}}$ | $\boldsymbol{m_{14} = 2b_{1-} = 2b_{1+}}$ |
| $\boldsymbol{m_{21} = a_{20}}$ | $\boldsymbol{m_{22} = a_{21}}$ | $\boldsymbol{m_{23} = 2a_{2-} = -2a_{2+}}$ | $\boldsymbol{m_{24} = 2b_{2-} = 2b_{2+}}$ |
| $\boldsymbol{m_{31} = a_{30}}$ | $\boldsymbol{m_{32} = a_{31}}$ | $\boldsymbol{m_{33} = 2a_{3-} = -2a_{3+}}$ | $\boldsymbol{m_{34} = 2b_{3-} = 2b_{3+}}$ |
| $\boldsymbol{m_{41} = a_{40}}$ | $\boldsymbol{m_{42} = a_{41}}$ | $\boldsymbol{m_{43} = 2a_{4-} = -2a_{4+}}$ | $\boldsymbol{m_{44} = 2b_{4-} = 2b_{4+}}$ |

Where ‘N’ is the number of the line taken from the image; $a_{\mathrm{N0}}$, $a_{\mathrm{N1}}$, $a_{\mathrm{N+}}$, $a_{\mathrm{N-}}$ are the real Fourier coefficient and $b_{\mathrm{N-}}$ and $b_{\mathrm{N+}}$ are the imaginary Fourier coefficient; $m_{\mathrm{ij}}$ are the 16 Mueller matrix component of the sample.

Here we have succeeded to determine all 16 elements of the Mueller matrix of the sample in a single shot. Channeled spectrum polarimetry using two high order retarders has been used with a circular grating. Circular grating divides the beam according to wavelength in a radial manner. Achromatic axially symmetric waveplate has a variation of azimuthal angle over space but retardance is constant. And as it is achromatic, it does not depend on the wavelength.

As this method is a single shot, using a high-speed camera it can be used as real-time measurement.

## 4.3 Experimental setup approach

To build up the system we needed a circular grating. It is not possible to work with conventional linear grating for this algorithm. Because here we have to take five spectra instead of one. The required grating type has been shown in Figure 4.2 below:

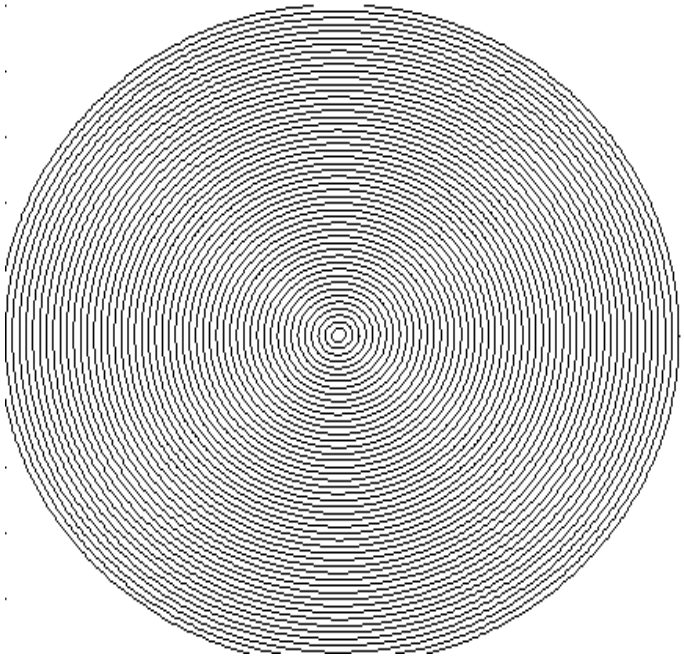

Fig 4.5 Circular grating diagram

Here is the diagram of a circular grating.

But we need only 5 directions of the circular grating. Therefore, instead of circular grating, we made a compound grating that has a linear grating in 5 directions. The diagram is shown in Figure 4.6

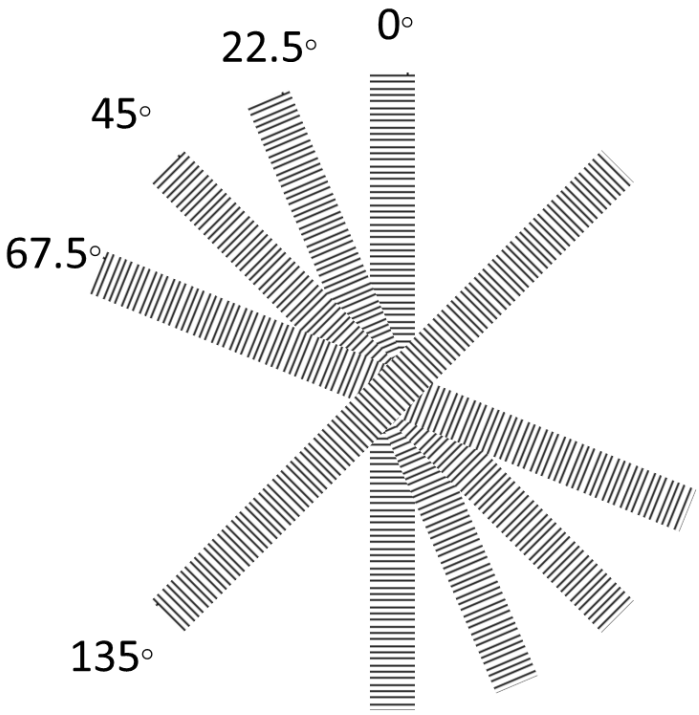


Fig 4.6Compound grating diagram

**500 lines** per mm sheet grating have been used to make this grating and it has catted and pasted in the proper direction. The picture of the grating is shown in figure 4.7.

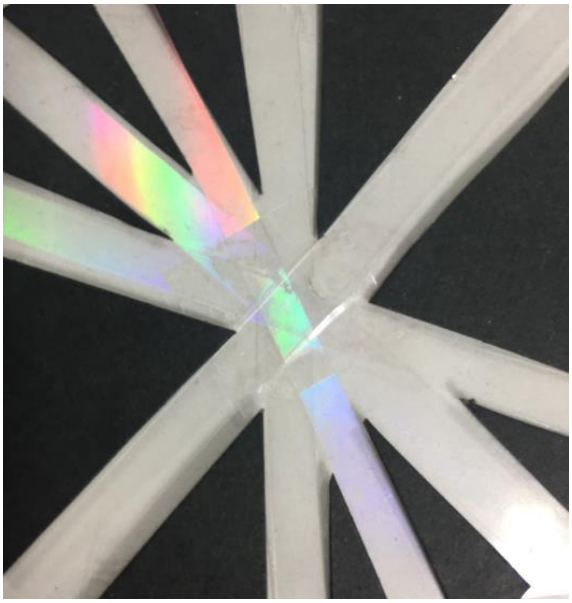

Fig 4.7Compound grating picture

The spectrum obtained by this grating is taken on a white screen. The spectrum we obtained on the screen is shown in Figure 4.8.

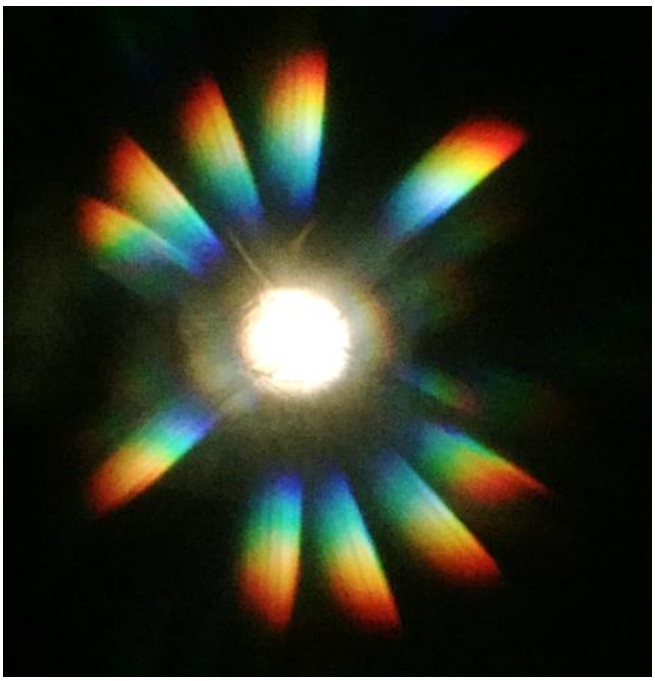

Fig 4.8spectrum obtained in the screen without focusing lens.

In our proposed technique, we are taking the upper half of the image, as the lower half is the reciprocal of the upper half. After focusing on a 40mm aromatic lens, the image has been obtained in the CCD camera as shown in Figure 4.9.

Fig 4.9 spectrum obtained in CCD after focusing on a 40mm achromatic lens.

# Conclusions

The enhancement of the Mueller matrix polarimeter is presented. Enhancement of accuracy is presented by the algorithm along with the supportive experimental results. Enhancement in time is described by the algorithm as it is a new theoretical approach.

In enhancement of accuracy, a calibration method for diattenuation and retardance errors for dual rotating retarder polarimeter is presented. The main objective to compensate the errors due to imperfect retarders to enhance the increment of accuracy. As any azimuthal errors have not considered, so to apply this algorithm it is necessary to align the retarders and analyzer properly. Based on the experimental results we can conclude that by the proposed method an increment of accuracy is obtained.

In the enhancement of time, we have succeeded to determine all 16 elements of the Mueller matrix of the sample in a single shot. Channeled spectrum polarimetry using two high order retarders has been used with a circular grating. Circular grating divides the beam according to wavelength in a radial manner. Achromatic axially symmetric wave plate has a variation of azimuthal angle over space but retardance is constant. And as it is achromatic, it does not depend on the wavelength.

As this method is a single shot, using a high-speed camera it can be used as real-time measurement.

# Reference


[1] R. M. A. Azzam, “Photopolarimetric measurement of the Mueller matrix by Fourier analysis of a single detected signal”, Opt. Lett., **2(**6), 148-150, (1978).

[2] D. H. Goldstein, “Mueller matrix dual-rotating retarder polarimeter”, Appl. Opt., **31**(31), 6676-6683, (1992).

[3] E. Compain, and B. Drevillon. "Complete high-frequency measurement of Mueller matrices based on a new coupled-phase modulator." Review of Scientific Instruments **68**(7), 2671-2680, (1997).

[4] E. G. Caurel, A. D. Martino, and B. Drevillon. "Spectroscopic Mueller polarimeter based on liquid crystal devices." Thin Solid Films **455**, 120-123, (2004).

[5] B. L. Boulesteix, A. D. Martino, B. Drévillon, L. Schwartz. "Mueller polarimetric imaging system with liquid crystals." Appl. Opt., **43**(14), 2824-2832, (2004).

[6] S. Y Lu, R. A Chipman, “Interpretation of Mueller matrices based on polar decomposition”, J. Opt. Soc. Am. A, **13(**5),1106-1113, (1996).

[7] D. Goldstein, “Polarized light”, (Marcel Dekker, Inc., 2003).

[8] R. A. Chipman, “Polarimetry,” in *Handbook of Optics*, (McGraw-Hill Professional, 1995), Chapter 22.

[9] N. Ghosh, I. A. Vitkin, "Tissue polarimetry: concepts, challenges, applications, and outlook." J. Biomed. Opt. **16(**11), 110801-11080129, (2011).

[10] N. Ghosh, M. F. Wood, I. A. Vitkin. "Mueller matrix decomposition for extraction of individual polarization parameters from complex turbid media exhibiting multiple scattering, optical activity, and linear birefringence." J. Biomed. Opt. **13**(4), 044036-044036, (2008).

[11] M. Sun, H. He, N. Zeng, E. Du, Y. Guo, S. Liu, J. Wu, Y. He, H. Ma. "Characterizing the microstructures of biological tissues using Mueller matrix and transformed polarization parameters." Biomed. Opt. Express 5.12 (2014): 4223-4234.

[12] M. Anastasiadou, A. D Martino, D. Clement, F. Liège, B. L. Boulesteix, N. Quang, J. Dreyfuss, B. Huynh, A. Nazac, L.Schwartz, and H. Cohen, "Polarimetric imaging for the diagnosis of cervical cancer." Physica Status Solidi (c), **5(**5), 1423-1426, (2008).

[13] S. Manhas, M. K. Swami, P. Buddhiwant, N. Ghosh, P. K. Gupta, and K. Singh, "Mueller matrix approach for determination of optical rotation in chiral turbid media in backscattering geometry." Opt. Express **14**(1), 190-202, (2006).

[14] J. M. Schmitt, A. H. Gandjbakhche, and R. F. Bonner, “Use of polarized light to discriminate short path photons in a multiply scattering medium,” Appl. Opt. **31**, 6535–6546 (1992).

[15] V. Sankaran, J. T. Walsh Jr., and D. J. Maitland, “Comparative study of polarized light propagation in biological tissues,” J. Biomed. Opt. **7**, 300–306 (2002).

[16] D. H. Goldstein, R. A. Chipman, “Error analysis of a Mueller matrix polarimeter”, J. Opt. Soc. Am. A, **7(**4), 693-700, (1990).

[17] P. S. Hauge, "Mueller matrix ellipsometry with imperfect compensators." J. Opt. Soc. Am. A,**68(**11),1519-1528, (1978).

[18] S. M. F. Nee, "Error analysis for Mueller matrix measurement." J. Opt. Soc. Am. A, **20**(8), 1651-1657, (2003).

[19] K. M. Twietmeyer, and R. A. Chipman. "Optimization of Mueller matrix polarimeters in the presence of error sources." Opt. Express **16**(15), 11589-11603, (2008).

[20] L. Broch, A. E. Naciri, and L. Johann. "Systematic errors for a Mueller matrix dual rotating compensator ellipsometer." Opt. Express **16**(12), 8814-8824, (2008).

[21] K. Bhattacharyya, D. I. S García, Y. Otani, “Mueller matrix polarimeter with diattenuation error calibration approach”, in *Proceedings of Advances in Optical Science and Engineering,* Springer India, **166**, pp 363-373, (2015).

[22] Chipman, R.A., “Polarimetry, Chapter 22, Handbook of Optics, Volume- II, Second Edition”, McGraw-Hill Professional, (1995).

[23] Okabe, Hiroshi, et al. "Spectroscopic polarimetry using channeled spectroscopic polarization state generator (CSPSG)." *Optics express* 15.6 (2007): 3093-3109.

[24] Wakayama, Toshitaka, et al. "Achromatic axially symmetric wave plate."*Optics express* 20.28 (2012): 29260-29265.

[25] Hagen, Nathan, Kazuhiko Oka, and Eustace L. Dereniak. "Snapshot Mueller matrix spectropolarimeter." *Optics letters* 32.15 (2007): 2100-2102.

**PAPERS:**

- K. Bhattacharyya, D.I.S García and Y. Otani, “Accuracy Enhancement of Dual Rotating Mueller Matrix Imaging Polarimeter by Diattenuation and Retardance Error Calibration Approach”. Optics Communications, 392, 48-53, 2017.

- K Bhattacharyya, Y Otani. “Single shot Mueller matrix polarimetry using axially symmetric quarter wave plate and channeled spectrum”. Optik. 2019, 183, 451-4.

- K. Bhattacharyya, D. I. S García, Y. Otani, “Mueller matrix polarimeter with diattenuation error calibration approach”, in *Proceedings of Advances in Optical Science and Engineering,* Springer, 166, pp 363-373, (2015).

## CONFERENCES:

- IEM OPTRONIX, Kolkata, 2014.
  K. Bhattacharyya, D. I. S. García and Y. Otani, “Mueller matrix polarimeter with diattenuation error calibration approach”.

- International Symposium on Optomechatronic Technology (ISOT), 2016.
  K. Bhattacharyya, N. Hagen, T. Wakayama and Y. Otani, “Single shot Mueller matrix polarimetery using axially symmetric quarter wave plate and channelled spectrum”.

- The Japan Society of Applied Physics (JSAP), Tokyo, 2016.
  K. Bhattacharyya, D. I. S. García and Y. Otani, “Mueller matrix polarimeter with non-ideal retarder calibration”.